What Drives Plate Motion?

Yongfeng Yang[1]

[1]Bureau of Water Resources of Shandong Province

November 30, 2022

Abstract

Plate motion is a remarkable Earth process and is widely ascribed to two primary driving forces: slab pull and ridge push. With the release of the first- and second-order stress fields since 1989, a few features of tectonic stresses provide strong constrain on these forces. The observed stresses are mainly distributed on the uppermost brittle part of the lithosphere. A modeling analysis, however, reveals that the stress produced by ridge push is dominantly distributed in the lower part of the lithosphere; Doglioni and Panza recently made an in-depth investigation on slab pull and found this force cannot be in accordance with observations. These findings of ridge push and slab pull suggest that there needs other force to be responsible for plate motion and tectonic stress. Here, we propose that the pressure of deep ocean water against the wall of continent yields enormous force (i.e., ocean-generated force) on the continent. The continent is fixed on the top of the lithosphere, this attachment allows ocean-generated force to be laterally transferred to the lithospheric plate. We show that this force may combine other forces to form force balances for the lithospheric plate, consequently, the African, Indian, South American, Australian, and Pacific plates obtain a movement of 4.52, 6.09, 2.11, 3.52, and 6.62 cm/yr, respectively. A torque balance modelling shows that the error between the movements calculated for 121 sample locations and the movements extracted from GSRM v.2.1 is less than 0.8 mm/yr in speed and 0.3o in azimuth.

Yongfeng Yang

Bureau of Water Resources of Shandong Province

Corresponding author: Yongfeng Yang (roufeng_yang@yahoo.com; roufeng_yang@outlook.com)

Key Points:

- Plate driving force provides the first insights into the processes that yield plate tectonics
- We investigate to find that the two primary driving forces (ridge push and slab pull) cannot be accordance with observation
- An ocean-generating force driving mechanism is proposed to account for plate motion

Abstract

Plate motion is a remarkable Earth process and is widely ascribed to two primary driving forces: slab pull and ridge push. With the release of the first- and second-order stress fields since 1989, a few features of tectonic stresses provide strong constrain on these forces. The observed stresses are mainly distributed on the uppermost brittle part of the lithosphere. A modeling analysis, however, reveals that the stress produced by ridge push is dominantly distributed in the lower part of the lithosphere; Doglioni and Panza recently made an in-depth investigation on slab pull and found this force cannot be in accordance with observations. These findings of ridge push and slab pull suggest that there needs other force to be responsible for plate motion and tectonic stress. Here, we propose that the pressure of deep ocean water against the wall of continent yields enormous force (i.e., ocean-generated force) on the continent. The continent is fixed on the top of the lithosphere, this attachment allows ocean-generated force to be laterally transferred to the lithospheric plate. The net effect of this force pushes the lithospheric plate. A semi-analytical model shows that this force may combine collisional force, shear force, and basal friction force to form force balance for the lithospheric plate, consequently, the African, Indian, South American, Australian, and Pacific plates obtain a movement of 4.52, 6.09, 2.11, 3.52, and 6.62 cm/yr, respectively.

Plain Language Summary

Plate tectonics is one of the most significant paradigms in the 20^{th} century, it mainly describes the movements of a dozen different-sized plates over the Earth's surface. Exploring the plate driving forces is fundamental because it provides the first insights into the processes that yield plate tectonics. Slab pull and ridge push are presently thought to be the two primary driving forces. In this study, we model a vertical distribution of the stress caused by ridge push and recall the geometric, kinematic, and mechanical arguments of slab pull. These findings suggest these forces cannot be in accordance with observations and other force is needed. Approximately 71% of the Earth's surface is covered with ocean water. Ocean water exerts pressure everywhere, this pressure against the walls

of continents creates enormous force on continents. In this study, we investigate the geometry of this force and its distribution around the lithospheric plates. By a semianalytical model, we find this force may combine collisional force, shear force, and basal friction force to form force balance for plate, consequently, plate motion can be realized.

1 Introduction

One of the most significantly achievements in the 20^{th} century was the establishment of the plate tectonics , which developed from the previous concept of continental drift (Wegener, 1915 and 1924). Plate tectonics mainly describes the motion of a dozen different-sized plates that connect with each other to form a giant "jigsaw puzzle" over the Earth's surface. The evidence supporting this motion includes shape fitting of the African and American continents, a coal belt crossing from North America to Eurasia, identical directions of ice sheet movement in southern Africa and India, and speed measurements made by the Global Positioning System (GPS). In addition, paleomagnetic reversals in oceans (Hess, 1962; Vine and Matthews, 1963) reflect sea-floor spreading, and studies of the Hawaii-Emperor seamount chain have shown that the chain is actually a trace of the lithosphere rapidly moving over relatively motionless hotspots (Wilson, 1963; Raymond et al., 2000), which further confirms the Earth's surface motion. During the past 50 years, the understanding of plate motion has expanded greatly. Plates were found to have been periodically dispersed and aggregated in the Mesozoic period, accompanied by 5-6 significant astronomical events (Cande and Kent, 1992; Cande et al., 1989; Ma et al., 1996; Wan, 1993; Hibsch et al., 1995). The speed and direction of plate motion supported by paleomagnetism and deformation in the intraplate regions exhibited various styles over geological time (Wan, 2018). Global measurements of tectonic stresses revealed a strong correlation with plate motion, and the observed stresses may be used to constrain the forces that act on the plates (Zoback et al., 1989; Zoback, 1992; Bott and Kusznir, 1984; Zoback & Magee, 1991; Richards, 1992; Sperner et al., 2003; Heidbach et al., 2016; Heidbach et al., 2007; Heidbach et al., 2010; Heidbach et al., 2018).

Exploring the plate driving forces is important because it provides the first insights into the processes that yield plate tectonics. Throughout the history of plate tectonics, a large number of forces have been postulated to explain plate motion. Forces include centrifugal and tidal forces, ridge push, slab pull, basal drag, slab suction, mantle plume, geoid deformation, and the Coriolis force (Wegener, 1915; Hales, 1936; Holmes, 1931; Pekeris, 1935; Runcorn, 1962a,b; Wilson, 1963; McKenzie, 1968; McKenzie, 1969; Morgan, 1971; Morgan, 1972; Turcotte and Oxburgh, 1972; Forsyth & Uyeda, 1975; Oxburgh and Turcotte, 1978; Spence, 1987; White & McKenzie, 1989; Richards, 1992; Vigny et al., 1992; Bott, 1993; Tanimoto & Lay, 2000; Conrad & Lithgow-Bertelloni, 2002; Turcotte and Schubert, 2014). Slab pull is derived from a cold and dense sinking plate that uses its weight to pull the remaining plate to which it is attached. Ridge push is usually treated either as a boundary force or a body force . As a

boundary force, ridge push is derived from a "gravity wedging" effect of warm, buoyant mantle upwelling beneath the ridge crest and acts at the edge of the lithospheric plate. In contrast, as a body force, ridge push is derived from the horizontal pressure gradient of the cooling and thickening of the oceanic lithosphere and acts over the area of the oceanic portion of a given plate. As these two forces act on the edges of plates, they are often termed boundary forces. Basal drag (i.e., basal shear traction) is thought to be caused by the viscous moving asthenosphere along the bottom of the lithosphere. Mantle plume represents the rising hot mantle flow that originated from the core-mantle boundary (Morgan, 1971; Morgan, 1972; Wilson, 1963). Early studies of deformation modeling and torque balance analysis tended to agree that ridge push and slab pull are important for plate motion, whereas basal drag provides resistance instead of driving force (Forsyth & Uyeda, 1975; Solomon et al., 1975; Chapple and Tullis, 1977; Richardson et al., 1979; Wortel and Cloetingh, 1981; Cloetingh and Wortel, 1986; Richardson and Cox, 1984; Richardson and Reding, 1991; Stefanick and Jurdy, 1992). Subsequent researches with complicated physical models yielded an improved understanding: buoyancy anomalies within the lithosphere, crust, , and mantle act as the principal drivers, whereas viscous dissipation within the lithosphere and at its base and shear along thrust faults at collision zones resist plate motion (Conrad and Hager, 1999; Conrad and Lithgow-Bertelloni, 2002; Stadler et al., 2010; Lithgow-Bertelloni and Richards, 1995; Becker and O'Connell, 2001; Zhong, 2001; Bird et al., 2008; Becker and Faccenna, 2011; Ghosh et al., 2013; Coltice et al., 2017). That is, besides slab pull and ridge push, the lithosphere and mantle feed plate motion in some way. For example, the lithosphere's density variation forms a lateral pressure gradient by which plate motion is driven. The sinking slab inserts into the deeper mantle while the hot mantle flows (i.e., plumes) originated from the core-mantle boundary rise up to the top of the asthenosphere; this process of upwelling and downwelling causes the large-scale circulation of plate and mantle (i.e., whole mantle convection). A more detailed description of whole mantle convection is discussed in these works (Coltice et al., 2017; Bercovici et al., 2015). On the whole, the efforts made in the past 40 years tend to agree that ridge push and slab pull are the primary plate driving forces, whereas mantle plumes that act as a driving force still remains controversial.

2 What's the problem of the primary driving forces

2.1 Ridge push

Tectonic stresses are caused by the forces that act on the plates (Middleton and Wilcock, 1996), and they in turn provide constrain on the plate driving forces. With the first release of the first- and second-order stress fields (Zoback et al., 1989; Zoback, 1992; Zoback & Magee, 1991), it becomes evident in the World Stress Map (WSM) that the maximum horizontal compressional stress S_H in North America, South America and Europe has the orientation that is predominately subparallel to either the relative or absolute plate motions (Richardson, 1992; Müller et al., 1992; Zoback, 1992). Due to this coupling of stress orienta-

tions and plate motions, the first-order intraplate stress patterns are concluded, mainly by means of torque analysis, to be caused by the same forces that drive plate motion, especially slab pull, ridge push, collisional forces, trench suction, and traction at the base of the lithosphere (Richardson, 1992; Zoback, 1992; Grünthal and Stromeyer, 1992; Gölke and Coblentz, 1996;Zoback and Zoback, 1991; Zoback and Burke, 1993; Zoback et al., 1989). Subsequent releases of the stress field (Heidbach et al., 2016; Sperner et al., 2003; Heidbach et al., 2010; Heidbach et al., 2007; Heidbach et al., 2018) and modeling studies that reproduce plate tectonics (Ghosh et al., 2013; Richards, 1992; Stadler et al., 2010; Becker and O'Connell, 2001; Bird et al., 2008; Ghosh and Holt, 2012; Lithgow-Bertelloni and Guynn, 2004; Alisic et al., 2012;) agree with this conclusion. Yet, this match in orientation and style (i.e., compressional or extensional) between the stresses produced by these forces and the observed stresses is limited to the lithosphere's surface, i.e., the lithosphere is treated as a thin "shell" that is similar to membrane, the related forces are acted at the edges of the lithospheric plates and their base to produce the stresses, the resultant stresses are projected on the surface of the plate, and then, these stresses are compared with the observed stresses in the WSM. Consequently, an examination of the consistency between the produced stresses and the observed stresses across the entire thickness of the lithosphere is commonly absent. In fact, the first release of the first- and second-order stress fields (Zoback et al., 1989; Zoback, 1992; Zoback & Magee, 1991) revealed another important feature of the tectonic stresses: the observed stresses are mainly concentrated on the uppermost brittle part of the lithosphere (which is ~ 40 km depth), except for some portions of the continent dominated by high topography. This vertical distribution feature of tectonic stresses is often not included by these modeling studies (i.e., Ghosh and Holt, 2012; Lithgow-Bertelloni and Guynn, 2004). As mentioned above, ridge push is treated either as a boundary force or a body force . As a boundary force, it is derived from a "gravity wedging" effect of warm, buoyant mantle upwelling and acts at the edge of the lithospheric plate. Relying on a model that is similar to Figure 1 (top), Turcotte and Schubert (2002) expressed ridge push force as F_{RP}=g $_m$ $_v$(T_1-T_0)[1+2 $_m$ $_v$(T_1-T_0)/ ($_m$- $_w$)] t, where g, $_m$, $_w$, T_1, T_0, $_v$, , and t are respectively gravitational acceleration, mantle density, water density, mantle temperature, temperature at plate surface, thermal expansivity, diffusivity, and age of seafloor. Since this expression was made through some mathematic substitution and integrations, and both mantle density and mantle temperature linearly increase with depth, these aspects determine that ridge push force would increase with depth. In other words, the minimum ridge push force, which is zero due to T_1= T_0, would appear at the top of the oceanic ridge, whereas the maximum ridge push force would appear at the bottom of the oceanic ridge. We here employ a simple model (Figure 1 (bottom)) to examine the vertical distribution of the stresses produced by ridge push force. The model consists of continental Plate A and oceanic Plate B. The plates are straight meaning the Earth's curvature is not considered. Plate A is assumed to be homogeneous and isotropic, and its thickness is given as 100 km. Along the horizontal direction, Plate B exerts a collisional force F_c on Plate A, this

force is resistive and uniformly exerted on the section *GH* of 90 km length; the oceanic ridge exerts a push force F_{RP} on the section *JI* of 85 km length, this force is driving and increases with depth; the mantle exerts a friction force F_b on the base of Plate A, this force is resistive and shears the section *HI* of 5000 km length. These forces realize a horizontal force balance for the section *GHIJ*. Along the vertical direction, Plate A is supported by the mantle, its gravity is balanced out by the supporting force from the mantle. Finite element analysis software (i.e., Abaqus) is used to resolve the resultant stress across the section *GHIJ*. The bottom of the section *GHIJ* is given a remote boundary condition. As the upper part of the lithospheric plate is elastic and brittle whereas the lower part is plastic and ductile, this reality allows us to assume that the physical property of section *GHIJ* is vertically transited from elasticity to plasticity. The inputs include the vertical pressure caused by the section *GHIJ*'s weight and the lateral pressures caused these forces F_{RP}, F_{b}, and F_{c}. The outputs include two sets of data: one is the stress produced by the vertical pressure alone, and the other is the stress produced by a combination of the vertical pressure and lateral pressures. The two-dimensional frame allows us to obtain a horizontal stress S11 and a vertical stress S22. Elastic modulus, Poisson ratio, and the rock's density of the section *GHIJ* are given as 100,000 Mpa, 0.3, and 2,690 kg/m^3, respectively. F_{RP} is given as 4.0×10^{12} N m^{-1}, this amplitude is generally accepted (Turcotte and Schubert, 2004). F_b and F_c are assumed to be 80% and 20% of the F_{RP}, which are 3.2×10^{12} N m^{-1} and 0.8×10^{12} N m^{-1}. To test a variation of the resultant stresses when the resistive forces are adjusted, F_b and F_c are again assumed to be 50% and 50% of the F_{RP}, which are 2.0×10^{12} N m^{-1} and 2.0×10^{12} N m^{-1}. And then, these forces are applied to the related sections, resulting in pressures. The produced stresses are exhibited in Figure 2. We find that the maximum horizontal stress S11 is compressional and mostly concentrated on the lower part of the section *GHIJ*. This style is dominant even if the magnitude of both F_b and F_c is adjusted. Kusznir and Bott (1977) argued that, because of the ductile nature of the lower part of the lithosphere, there would be a redistribution of any stress applied to the whole lithosphere and result in a stress amplification in the upper brittle part of the lithosphere. This view is based on an assumption that force is uniformly exerted on the side of the lithospheric plate, but the reality is ridge push force would increase with depth, consequently, the redistribution of the stress and its amplification are not applicable to ridge push force. Instead, we have considered the ductile nature in the modeling, but no evidence is found to show a stress amplification in the upper brittle part of the section *GHIJ*. This analysis of the vertical distribution of horizontal stress indicates that the stress caused by slab pull cannot be in accordance with the observed stress.

Look over the plate's shape around the globe, it is evident that the eastern coastline of the American continent is approximately subparallel to the Atlantic ridge where it is the plate's boundary, and the coastline of the Australia's continent is subparallel to the boundary of the Australian plate. However, the length of the coastline of the American continent is greater than that of the Atlantic

ridge, whereas the length of the coastline of the Australian continent is far less than that of the boundary. This pattern is also clear for the Indian plate. This discrepancy suggests that the plate driving force is likely to be a force arising from the coastline that pulls the continental plate rather than a force arising from the boundary (ridge) that pushes the continental plate.

All plates are steadily moving over the Earth's surface, this reality indicates that there are the separation and approach between plates. The separation would result in a gap between two plates. If the gap were deep enough, it would allow magma to erupt and form a mid-ocean ridge (MOR). In this respect, the MOR may be the result of plate motion. Nowadays, the MOR is treated as the cause of the plate driving force. This treatment leads to the chicken-or-egg question: which came first? In physics, the object that exerts force must clearly differentiate from the object that accepts this force. Some people argue that once subduction and spreading are initiated, plates may drive themselves as part of large circulation of the mantle and lithosphere, by which the chicken-or-egg question is resolved. This argument cannot be convincing. Ridge push contributes to not only oceanic plates but also continental plates, but continental plates are not sinking, they cannot take part in the large circulation, consequently, the chicken-or-egg question remains for the ridge push of continental plates.

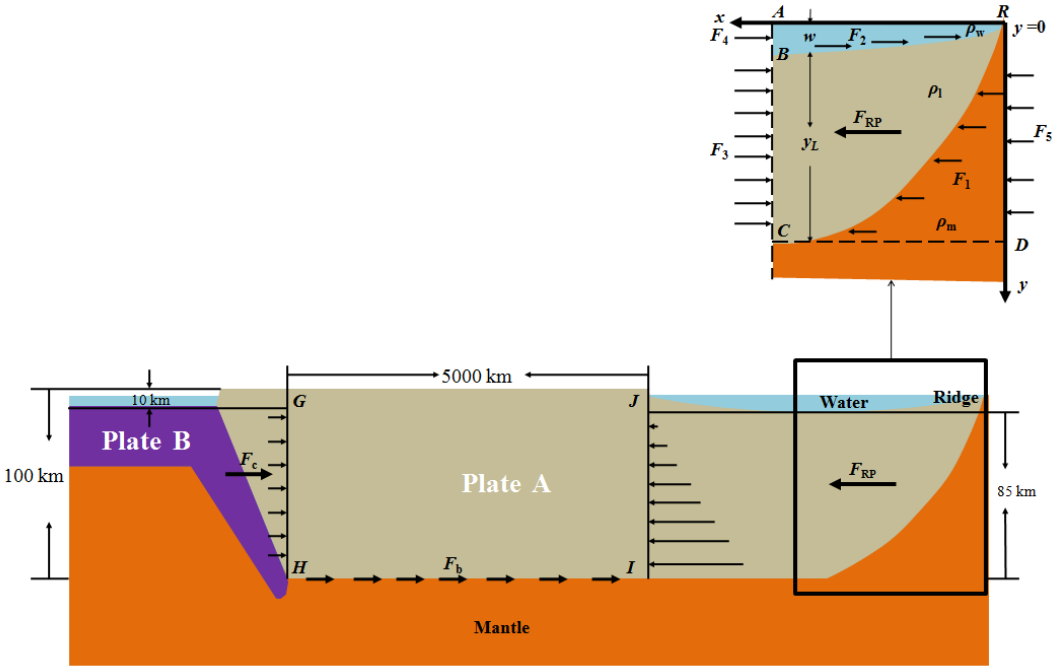

Figure 1. Modeling the distribution of ridge push, basal friction, and collsional force around a continental plate.

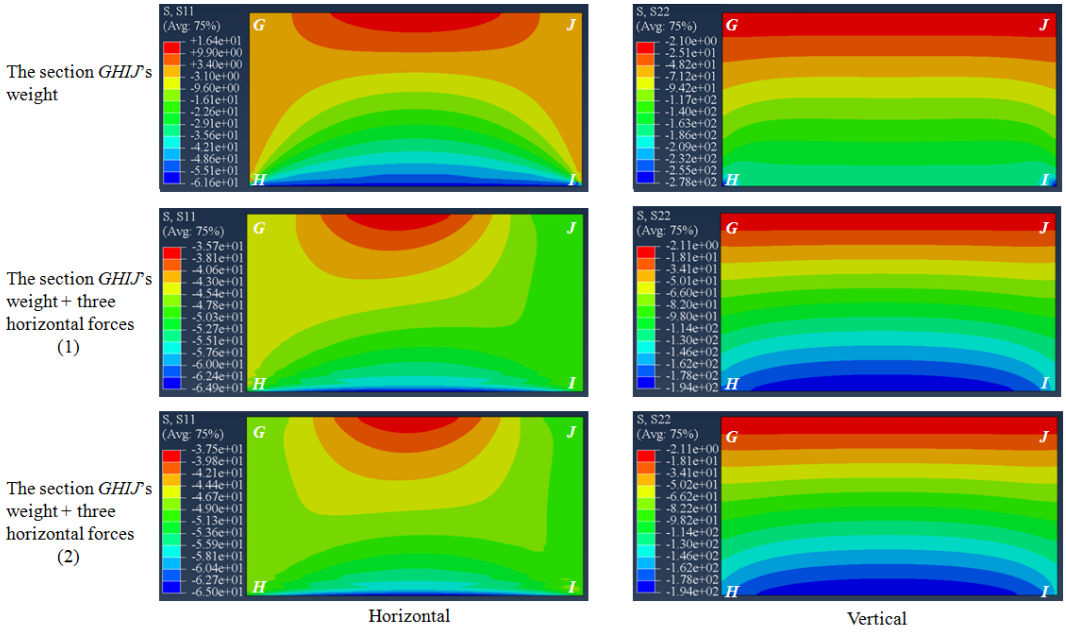

Figure 2. Stresses caused by a combination of ridge push, basal friction, and collisional force within a modelled section of continental plate. In the model of the section *GHIJ*'s weight + three horizontal forces (1), F_b and F_c are 80% and 20% of the F_{RP}, respectively; whereas in the model of the section *GHIJ*'s weight + three horizontal forces (2), F_b and F_c are 50% and 50% of the F_{RP}, respectively.

2.2 Slab pull

Slab pull is conceived as a "negative" buoyancy of sinking slab to drive the motion of the oceanic plate (e.g., Conrad & Lithgow-Bertelloni, 2003). However, since this force was proposed, its validity remains debated. Doglioni and Panza (2015) recently carried an in-depth investigation on slab pull, some of their findings include: 1) As demonstrated by Cruciani et al. (2005) that the slab's dip is unrelated to the age of the oceanic lithosphere, consequently, the negative buoyancy that increases with age and is determined by the cooling oceanic lithosphere cannot control the slab's dip; 2) It is assumed that the eclogitization within a slab would increase the lithosphere's density. Nevertheless, eclogitization is mostly distributed in the oceanic crust of 6~8 km depth, this transformation does not occur in the remaining lithospheric mantle of 60~80 km depth. It is possible that a little part of the slab's density can increase, but the majority of the slab's density does not change; 3) It is often asked why the lithosphere would subduct. This issue arises when an oceanic hydrated and serpentinized lithosphere is involved (Ulmer & Trommsdorff, 1995). Without being metamorphosed by the subduction process, the oceanic lithosphere would

not denser than the surrounding rocks. As pointed out by Panza et al.(2007), the serpentinized LID often occurs along transform faults and ridges, therefore, it is lighter than the asthenospheric mantle, a question is then how plates can be pulled? 4) Most of the slabs is affected by down-dip compression, this influence is limited to a depth of below 300 km (Isacks & Molnar, 1971). Frepoli et al. (1996) showed that most of slabs may appear at shallower depth, this situation requires a slab to be forced to sink rather than positively to sink; 5) Although there is no slab for continental plates, these plates still move, the movements of North America, South America, and Africa are the examples (Gripp & Gordon, 2002). Trench suction is widely used to account for these movements, but the mantle that is beneath both South and North America is moving eastward (Russo & Silver, 1994; Bokelmann, 2002), this trend is object to the kinematics required by the trench suction model; 6) In the hot spot reference frame it seem like that plate velocities are inversely proportional to the low velocity zone's viscosity and not related to both the age of the downgoing lithosphere and the length of the subduction zones. For example, the Pacific plate is the fastest moving plate, but the viscosity of the asthenosphere beneath this plate is rather low (Pollitz et al., 1998; Gripp & Gordon, 2002); 7) The vertical velocity of plates (subduction-related uplift or subsidence along plate boundaries) is far slower than the horizontal one (Kreemer et al., 2002), this situation implies that the vertical motions of plates are rather passive. Also, an analysis of kinematics reveals that subduction rate appears to be controlled by horizontal plate motion; For instance, along E- (or NE-) directed slabs, the convergence rate is faster than the subductionand, therefore the subduction cannot be the energetic source of plate motion; 8) When one addresses the plate motion relative to the underlying mantle, the slab might move out of the mantle, the slab is sinking just because there is faster upper plate which overrides it (El Gabryet al., 2013); 9) The strength of the oceanic lithosphere is low (e.g., about 8×10^{12} N m^{-1})(Liu et al., 2004), this reality means that the oceanic lithosphere is able to resist a force that is smaller than slab pull (about 3.3×10^{13} N m^{-1})(Turcotte & Schubert, 2002). If slab pull is the primary driving force for the Pacific plate, the argument of strength above would require a stretching for the Pacific plate before slab pull drives this plate to move; 10) Brandmayr et al. (2011) and El Gabry et al. (2013) recently investigated the geodynamis in the Mediterranean region. Their findings of Vs and distribution with depth suggest that slabs are less dense than the surrounding mantle and no evidence is found to support slab pull.

These arguments on slab pull leads to a conclusion that slab pull cannot drive the oceanic plate to move (Doglioni and Panza, 2015). This conclusion is further strengthened by Faccincani et al. (2021). These authors revealed the lithospheric mantle's density structure can be affected by the variations in thermal regimes and bulk composition, their results suggest that the lithospheric mantle is not denser than the underlying asthenospheric mantle. A difference of density between the lithospheric mantle and underlying asthenospheric mantle means that the oceanic plate, which mostly consists of the lithospheric mantle,

is unlikely to sink forming a "negative" buoyancy to drive plate motion.

As mentioned earlier in the section 1, the latest understanding of plate dynamics is that buoyancy anomalies within the lithosphere, crust, and mantle act as the principal drivers of plate motion. In short, the dynamic source of plate motion is ascribed to the crust, lithosphere, and mantle. The terrestrial planets (Venus, Mercury, and Mars) share similar formation procession and interior structure (i.e., crust, mantle, and core) with the Earth, and also undergo same spatial surrounding (i.e., asteroid impact) as the Earth does. Therefore a question is why there is plate motion on the Earth, except for these terrestrial planets? This discrepancy of plate motion distribution, together with these issues of ridge push and slab pull that we demonstrate above, implies that that some key factor of the Earth, which is still unrecognized to us today, determines plate motion.

3 An ocean-generating force driving mechanism for plate motion

Ocean water covers approximately 71% of the Earth's surface, and its total volume is almost 1.35 billion km^3, with an average depth of nearly 3,700 meters. Geochemical study of zircons suggests liquid water has existed for more than 4 Gy ago (Mojzsis et al., 2001; Bercovici et al., 2015; Valley et al., 2002). Ocean water is supported by the upper part of the lithosphere, this loading allows ocean water's weight to be vertically transferred to the lithosphere. The impact of ocean water on the isostatic balance and heat process of the lithosphere has been widely discussed (Bercovici et al., 2015; Fleitout and Froidevaux, 1983; Osei Tutu et al., 2018; Ricard et al., 1984; Steinberger et al., 2001; Lithgow-Bertelloni, 2014; Ghosh and Holt, 2012; Naliboff et al., 2012). The absence of plate tectonics on the other terrestrial planets (e.g., Mars and Venus) suggests that liquid water is related to plate tectonics, but the mechanism by which liquid water contributes to plate tectonics remains enigmatic. A view is the Earth's surface is cooled by liquid water, since the Earth's temperate in the formation of plate tectonics needs to be stabilized by a negative feedback (Bercovici et al., 2015; Walker et al., 1981; Berner, 2004). Nevertheless, from a view of fluid mechanics, ocean water (as liquid) can exert pressure everywhere, this pressure against the wall of the continent creates enormous force on the continent. As the continents are fixed on the top of the lithosphere, and the lithospheric plates connect to each other, this attachment of the continents to the top of the lithosphere allows this force to be laterally transferred to the lithospheric plates.

3.1 Forces acting on the continental plate

A liquid can exert pressure on the wall of a container that holds it. According to Figure 3, the pressure generated on the wall of a cubic container may be written as $P = \mathrm{g}y/2$, and the application of this pressure across the wall yields a force. This force may be expressed as $F = PS = \mathrm{g}y^2x/2$, where S is the wall's area, g and are the gravitational acceleration and liquid's density , respectively, and x and y are the liquid's width and depth, respectively, in the container. Referring to the real world, ocean basins are naturally gigantic containers, and their depths are often more than a few kilometers and vary from one place to another. All of these factors imply that oceans can generate enormous pressure everywhere and that this pressure is unequal among oceans. Furthermore, the application

of pressure against the ocean basin's walls, which consist of the continents, can yield enormous unequal forces on the continents. Geometrically, ocean pressure is always exerted vertical to the continental slope, by which a normal force is formed. This normal force is called ocean-generated force, which may be further decomposed into horizontal force and vertical force. As the continent attaches to the upper part of a continental plate, ocean-generated force can be laterally transferred to the continental plate. Subsequently, we list the plausible forces that act on a continental plate (Figure 1), and discuss the physical nature of these forces. These forces can be classified into two categories: the forces acting on the parts of the continent that connect to oceans and those acting at both the bottom surface of the continental plate and the parts of the continental plate that connect to adjacent plates. The forces acting on the parts of the continent that connect to the ocean derive from ocean pressure and are treated as ocean-generated forces, denoted F_R on the right and F_L on the left. The horizontal forces decomposed from these forces are denoted F_R' on the right and F_L' on the left. The force acting on the continental plate's bottom surface arises from a coupling between the plate and underlying viscous asthenosphere. It is called the basal friction force and denoted as f_{base}. As addressed by Forsyth & Uyeda (1975), if there is thermal convection in the asthenosphere, f_{base} would be a driving force (Runcorn, 1962a, b; Turcotte & Oxburgh, 1972; Morgan, 1972). If, instead, the asthenosphere is passive relative to plate motion, f_{base} would be a resistive force. Here, we assume f_{base} is a resistive force. The forces acting on the parts of the continental plate that connect to adjacent plates arise from a physical connection of the continental plate and adjacent plates. Given that the continental plate moves towards the right, they are called the collisional force from the plate on the right side, the shearing force from the plate on the far side, the shearing force from the plate on the near side, and they are denoted f_{right}, f_{far}, and f_{near}, respectively. Oceanic ridge represents a boundary of two separating plates, we assume there is no pull force from the plate on the left side. Then, a combination of all of these forces for the continental plate in the horizontal direction may be written as

$$F = (F_L\text{'} - F_R\text{'}) - (f_{base} + f_{right} + f_{far} + f_{near}) \quad (1)$$

where the first term (F_L'- F_R') denotes the final horizontal force, which provides a dynamic source for the continental plate, the second term (f_{base}+ f_{right} + f_{far}+ f_{near}) denotes the total resistive force, which hinders the continental plate's movement. Here, we indicate (F_L'- F_R') as F_{final} and (f_{base}+ f_{right} + f_{far}+ f_{near}) as $F_{resistive}$. F_L' and F_R' may be further written as $F_L\text{'}=0.5\ \mathrm{g}Lh_L^2$ and $F_R\text{'}=0.5\ \mathrm{g}Lh_R^2$, where , g, L, h_L, and h_R are the density of water, gravitational acceleration, ocean width that fits the continent's width, ocean depth at the left, and ocean depth at the right, respectively.

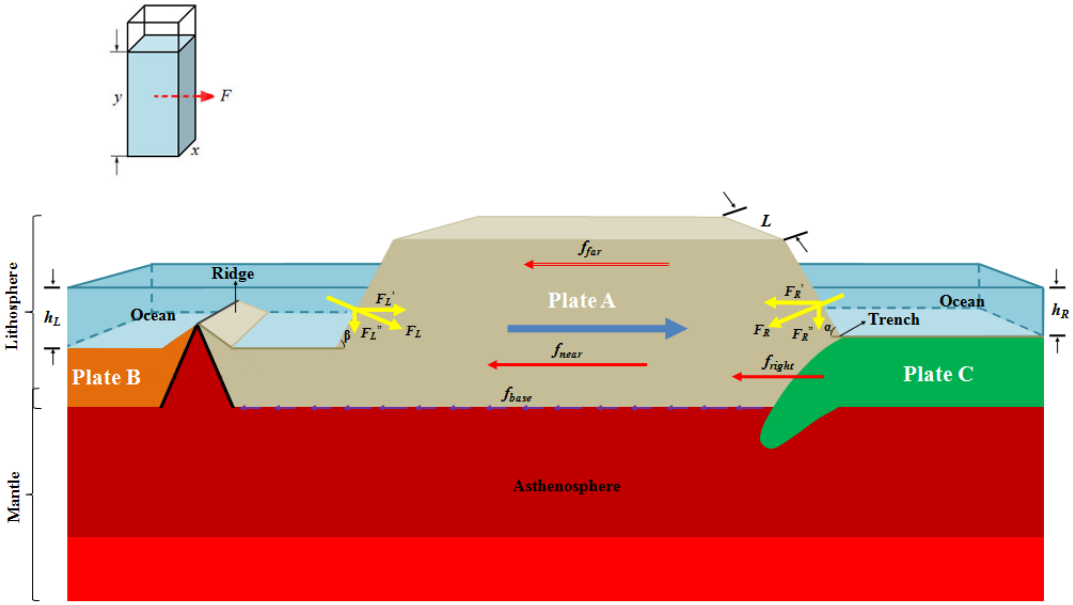

Figure 3. Modeling the dynamics of a continental plate. $F_L(F_R)$ represents the ocean-generated force on the left (right) side of the continental Plate A, while F_L'(F_R') and F_L''(F_R'') denote the horizontal and vertical forces decomposed from the ocean-generated force, respectively. Given Plate A moves towards the right (marked with blue arrow), the term f_{base} denotes the basal friction force exerted by the underlying asthenosphere, while f_{right}, f_{far}, and f_{near} denote the collisional force from Plate C on the right side, the shearing force from the plate on the far side, and the shearing force from the plate on the near side of Plate A, respectively. L denotes the width of the continent's side; h_L and h_R are the ocean's depth on the left and right, respectively. and denote the inclinations of the continent's slope on either side. Note that the ocean depth and the lithospheric plate's thickness are highly exaggerated.

3.2 Continental plate's motion

Equation (1) provides three possibilities for the continental plate. If the final horizontal force is greater than the total resistive force, the combined force is greater than zero, and the continental plate would be subjected to an accelerating motion. Practically, it is impossible for the continental plate to undergo such a movement. If the final horizontal force is equal to the total resistive force, the combined force is zero, and the continental plate would be subjected to a steady motion. If the final horizontal force is less than the total resistive force, the combined force is less than zero, and the continental plate would remain motionless. The total resistive force, as shown in Figure 3, includes three components: the basal friction force, collisional force, and shearing forces. Here, we separate the final horizontal force into two parts to exert: one, as an oppos-

ing force, balances the collisional force and shearing forces, and the other, as a driving force, balances the basal friction force. These balances of forces allow the plate's motion to be steadily maintained. The balance between the driving force and the basal friction force may be written as

$F_{driving}$ - f_{basal} = 0 (2)

where $F_{driving}$ denotes the driving force and f_{basal} denotes the basal friction force. The basal friction force exerted by the asthenosphere along the plate's base can be expressed as f_{basal} = Au/y, where , A, u, and y are the viscosity of the asthenosphere, the plate's area, the plate's speed, and the thickness of the asthenosphere, respectively.

In practice, the continent's side is not flat, and the continent's base is generally wider than its top, making the continent look more like a circular truncated cone standing in the ocean. As the horizontal force generated is related to the ocean's width (i.e., the continent side's width), we need to horizontally project the continent into a polygonal column, dissect the whole side of this column into a series of smaller rectangular sides connecting one to another and subsequently calculate the horizontal force generated at each of these rectangular sides. Here, four continental plates (South American, African, Indian, and Australian) are selected to demonstrate the horizontal forces and resultant movements (Figure 4). The longitude and latitude of the control sites (e.g., numbers 1, 2, 3, ...) determine the lengths of the continent's sides.

As the horizontal forces exerted on the continent's sides are often along different directions and the Earth's surface is curved, we need to combine these vector forces into a final horizontal force. To facilitate the following deduction, we employ a three-dimensional coordinate system and decompose each of the horizontal forces into three forces along the x, y, and z axis (Figure 5). Subsequently, by simple addition, all of the x, y, and z axis forces are separately combined into a total x axis force, total y axis force, and total z axis force. We further assume that each of these three total forces is exerted on the continent's geometric center, from where the total x axis force yields a latitudinal force, the total y axis force also yields a latitudinal force, and the total z axis force yields a longitudinal force. A simple addition of these two latitudinal forces represents a total latitudinal force, then, a combination of the total latitudinal force and the longitudinal force represents the final horizontal force. The final horizontal force may be written as $F_{final}=(F_{latitudinal}{}^2+F_{longitudinal}{}^2)^{0.5}$, where $F_{latitudinal}$ and $F_{longitudinal}$ are the total latitudinal force and the longitudinal force, respectively. The total latitudinal and the longitudinal forces can be expressed as $F_{latitudinal}$=-$F_x$sin +$F_y$cos , $F_{longitudinal}$=$F_z$cos , where F_x, F_y, and F_z denote the total x, y, and z axis force, respectively. These forces can be expressed as , , and , where $F_{i\text{-}x}$, $F_{i\text{-}y}$, and $F_{i\text{-}z}$ denote the x, y, and z axis force that are decomposed from the horizontal force generated at the ith side of the continent, $F_{i\text{-}x}$= -F_i(sin $_i$sin $_i$cos $_i$+cos $_i$sin $_i$), $F_{i\text{-}y}$= F_i (cos $_i$cos $_i$-sin $_i$sin $_i$sin $_i$), and $F_{i\text{-}z}$= F_i sin $_i$cos $_i$. $_i$ and $_i$ denote the longitude and latitude of the hypothetical center of geometry of the ith side, on which the horizontal force F_i is

exerted. They may be approximately represented by an average of the longitude and latitude of the two sites that are located at the two ends of the side, and can be written as $_i$=(d_M+d_N)/2 and $_i$=(q_M+q_N)/2, where d_M, d_N, q_M, and q_N denote the longitude and latitude of the two sites. $_i$ denotes the inclination of the horizontal force F_i to the latitudinal direction and can be obtained through the longitude and latitude of the two sites at the side. The horizontal force F_i may be written as F_i=0.5 g$L_i h_{i\text{-ocean}}{}^2$, and , g, L_i, and $h_{i\text{-ocean}}$ are the density of water, gravitational acceleration, length of the ith side, and the ocean depth that connects to the ith side. and denote the longitude and latitude of the hypothetical center of geometry of the continent, they may be approximately represented with the mean longitude and latitude of all the sites on the continent and can be written as , and , where d_j and q_j denote the longitude and latitude of the jth site, and n denotes the total number of sites. The parameters involved for the four selected plates and final calculated horizontal forces are separately listed in Tables 1 and 2.

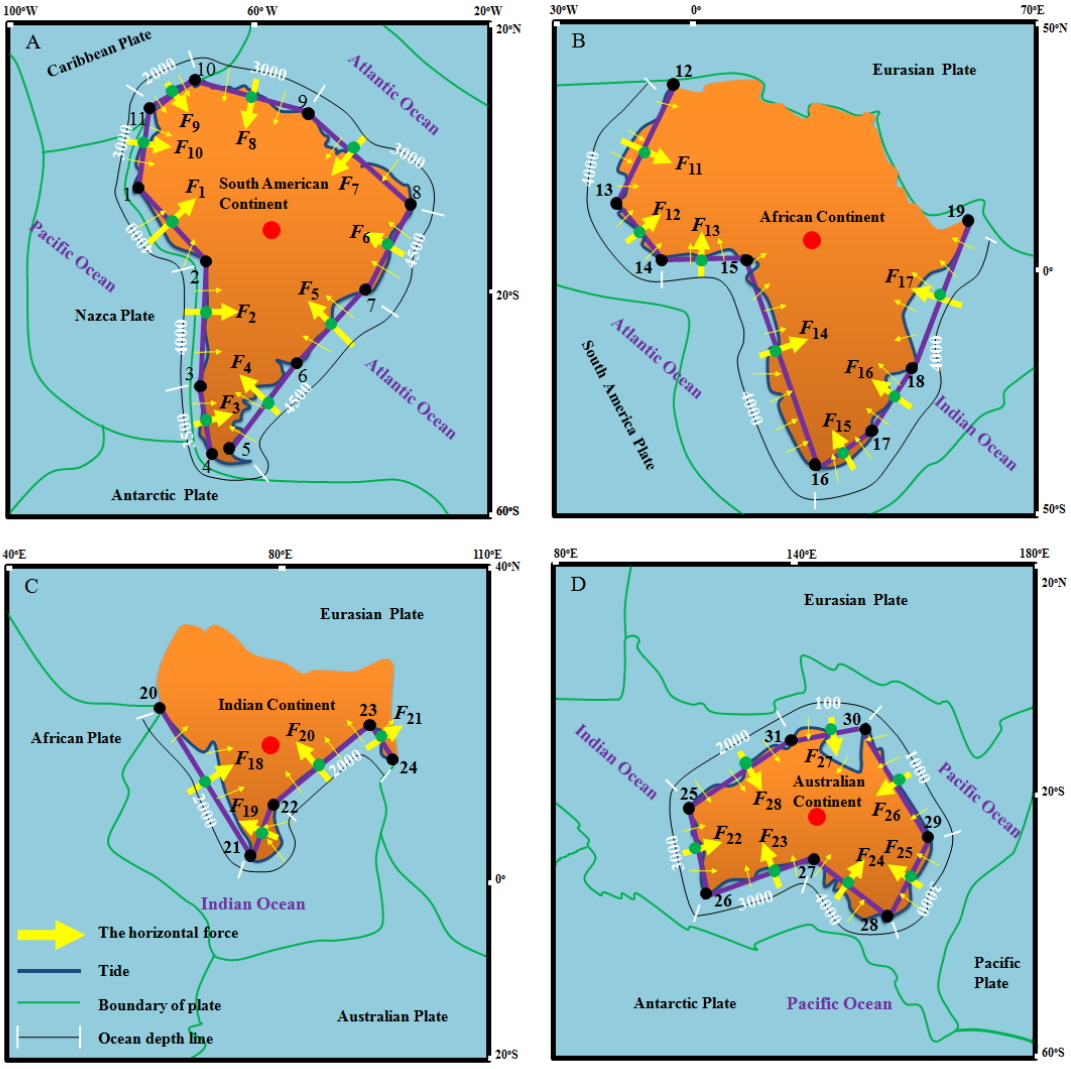

Figure 4. Geographic treatment of the control sites for the four selected continental plates and the horizontal forces generated for them. F (yellow arrows) denotes the generated horizontal force, while the purple bars denote the distances affected by the horizontal forces. The product of this distance and ocean depth is the area to which the horizontal force is applied. The black dots with numbers denote the control sites; the green dots denote the hypothetical centers of geometry of the sides; and the red dots denote the hypothetical centers of geometry of the continents. Ocean depths were artificially resolved from Google Earth software.

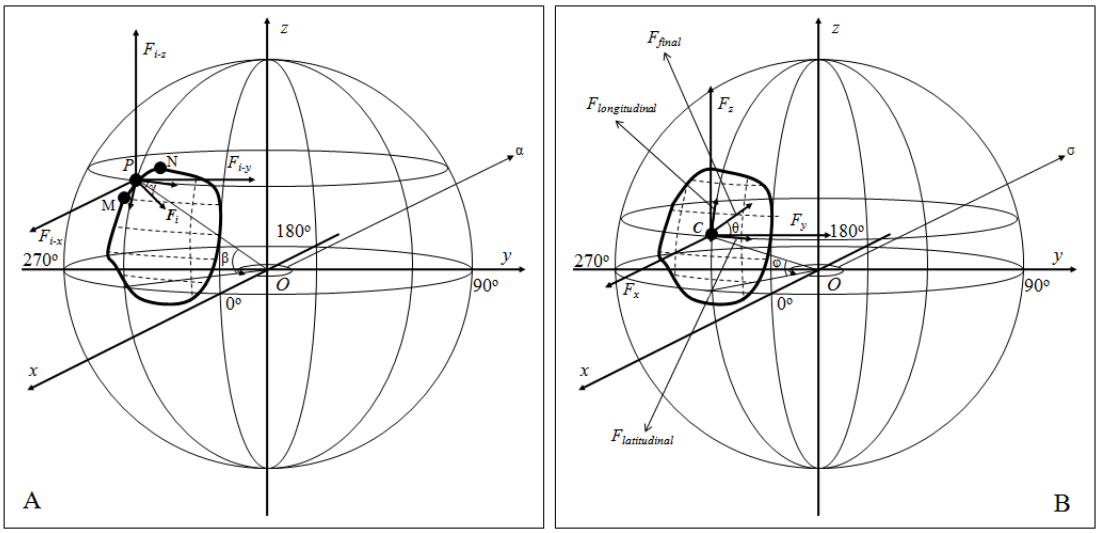

Figure 5. Modeling the vector force along the Earth's curved surface. (A) The horizontal force F_i is decomposed into the x axis force $F_{i\text{-}x}$, y axis force $F_{i\text{-}y}$, and z axis force $F_{i\text{-}z}$. Site P denotes the hypothetical center of geometry of the ith side (line MN, for instance) of a continent, on which the horizontal force F_i is exerted. and denote the longitude and latitude of the hypothetical center of geometry of the ith side. denotes the inclination of the horizontal force F_i to the latitudinal direction. **(B) The total x axis force F_x, total y axis force F_y, and total z axis force F_z are combined into a final horizontal force F_{final}.** $F_{latitudinal}$ and $F_{longitudinal}$ denote the latitudinal force and longitudinal force, respectively. Site C denotes the hypothetical center of geometry of the continent. and denote the longitude and latitude of the hypothetical center of geometry, and denotes the inclination of the final force F_{final} to the latitudinal direction.

Table 1 Basic information on the four selected continental plates

Plate	Area	Control site	Hypo
	S km^2	j	d$_j$ Long
South American	43,600,000	1	280.0
		2	290.0
		3	287.0
		4	287.0
		5	292.0
		6	306.0
		7	318.0
		8	326.0
		9	307.0

Table 1 Basic information on the four selected continental plates

		10	288.0
		11	282.0
African	61,300,000	12	353.6
		13	343.2
		14	352.7
		15	8.00
		16	22.20
		17	30.40
		18	40.00
		19	51.00
Indian	11,900,000	20	66.80
		21	77.50
		22	80.00
		23	91.50
		24	94.30
Australian	47,000,000	25	114.0
		26	117.2
		27	131.0
		28	149.8
		29	153.0
		30	142.4
		31	131.0

Notes: all geographic sites refer to Figure 4.

Table 2 Ocean-generated force for the selected continental plates

	i	horizontal F_i N (*10^{17})	decomposed $F_{i\text{-}x}$
South American	1	1.6362	1.3792
	2	0.9043	0.7892
	3	1.6686	1.5957
	4	2.2905	-1.1120
	5	1.7169	-0.4839
	6	1.9365	-0.8897
	7	1.1136	-0.4301
	8	0.951	-0.2098
	9	0.1639	0.1067
	10	0.4555	0.4373
			1.1825
African	11	1.9873	0.7267
	12	1.2000	0.0477
	13	1.3298	0.1043

Table 2 Ocean-generated force for the selected continental plates

	14	3.5882	-0.5695
	15	0.6949	0.4375
	16	1.4924	0.9846
	17	2.5379	1.7056
			3.4369
Indian	18	0.9724	-0.8284
	19	0.3729	0.3407
	20	0.6474	0.3396
	21	0.3531	-0.3231
			-0.4712
Australian	22	1.074	-0.9938
	23	1.6411	-0.1549
	24	2.2618	-1.3851
	25	0.6129	0.2125
	26	0.0965	0.0566
	27	0.0006	0.0000
	28	0.4237	-0.1335
			-2.3982

Note: all related forces refer to Figure 4.

The asthenosphere viscosity is not exactly determined. Many numerical studies using glacial isostatic adjustment and geoid modeling showed that the asthenospheric viscosity ranges from 10^{17} to 10^{20} Pa s (e.g., Steinberger, 2016; Hager and Richards, 1989; Mitrovica, 1996; King, 1995; Kido et al., 1998; James et al., 2009; Pollitz et al., 1998; Berker, 2017; Kaufmann and Lambeck, 2000; Hu et al., 2016;). Laboratory experiments, however, suggested that the magnitude of the asthenosphere viscosity could be substantially different from those constrained from numerical studies. The viscosity is variable and likely related to the thermodynamic state, grain size, composition of the medium, and state of stress (Bercovici et al., 2015). Both the melt contents of asthenosphere and the water in the asthenosphere may greatly affect the viscosity (Mei et al., 2002; Hirth and Kohlstedt, 1996). Hirth and Kohlstedt (1996) reported a variable viscosity profile for a melt-free oceanic lithosphere, the mean value of this viscosity profile is ~10^{18} Pa s. These authors (e.g., Doglioni et al., 2011; Scoppola et al., 2006) concluded that, in consideration of the water- and melt-rich layers characterized by much lower viscosities, a strong vertical variability of viscosity may be more realistic. The asthenosphere's effective viscosity can be greatly lowered to 10^{15} Pa s if water content in the case of both diffusion and dislocation creeps is included (Korenaga and Karato, 2008). Scoppola et al. (2006) made a more detailed review of the asthenosphere viscosity, and concluded that the presently accepted values of viscosity might be reduced through a combined experiment including these parameters (i.e., melt content, water content, mechanical asnisotropy, and shear localization). A "superweak", low-viscosity asthenosphere

supported by recent obsevations is being accepted by geophysical community (Kawakatsu et al., 2009; Hawley et al., 2016; Holtzman, 2016; Naif et al., 2013; Freed et al., 2017; Hu et al., 2016; Stern et al., 2015; Bercker, 2017). Jordan (1974) treated the asthenospheric thickness as 300 km. Taking into account the present status of the viscosity and thickness of the asthenosphere above, we adopt $=10^{18}$ Pa s and y=300 km, take the plate's area in Table 1 and the driving force $F_{driving}$, which is 60% of the final horizontal force F_{final} in Table 2, and use equation (2) to resolve the continental plate's speed, i.e., u= $F_{driving}$ y/ A. The movement's direction is represented with the direction of the final horizontal force and may be expressed as tan $= F_{longitudinal}/F_{latitudinal}$. The calculated movements for these plates are listed in Table 3.

The above treatment of the continental plate's motion is rather idealized. Because most of the horizontal forces exerted on the continental plate are along different directions and cannot pass the barycenter of the continental plate, this situation may produce a torque to rotate the continental plate. Figures 6 (A and B) conceptually demonstrate how these continental plates (North American and Eurasian, for example) move under the torque produced by the horizontal forces. A more detailed description about this torque effect cannot be included here and will be shown in another work.

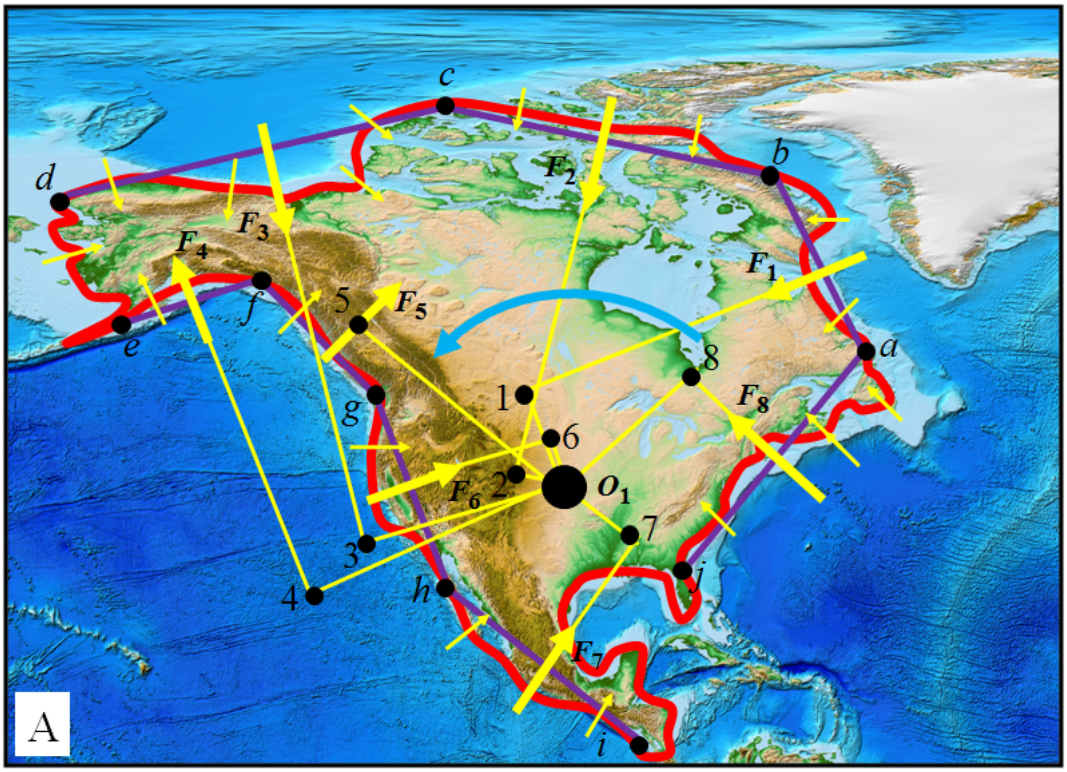

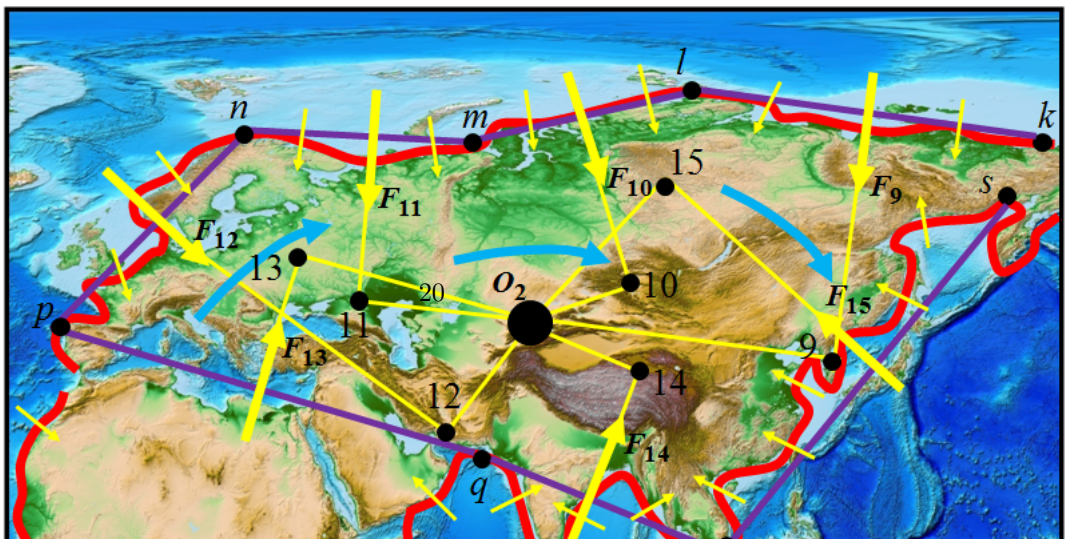

As mentioned earlier, a portion of the final horizontal force is used to oppose the collisional force from the plate on the right side, the shearing forces from the plate on the far side, and the shearing force from the plate on the near side. According to the principle of action and reaction, the final horizontal force pushes the plate on the right side, and shears the plates on the far and near sides.

The oceanic plate's motion can be realized by the force that transfers from the continental plate to the oceanic plate. This tranferring of force may be exemplified by the Pacific plate's motion. As outlined in Figure 7, we assume, by means of a force vector, that the North American plate provides a push force F_{PN} on the hypothetical center of geometry of the Pacific plate, and thatthe Australian plate provides a push force F_{PA} on the hypothetical center of geometry. The combination of these two forces is the final horizontal force F_P, which contributes to the dynamics of the Pacific plate. The other forces that act on the Pacific plate include the collisional force from the part of North American Plate and the Eurasian Plate, the basal friction force exerted by the underlying asthenosphere, the shearing force from the Australian plate, and the shearing forcefrom the North American plate. These other forces are denoted F_{far}, f_{base}, F_{right}, and F_{left} , respectively. As mentioned in section 3.1, we assume f_{base} to be a resistive force. And then, we separate the final horizontal force into two parts to exert: one, as an opposing force, balances the collisional force and shearing forces, and the other, as a driving force, balances the basal friction force. These balances of forces allow this plate's motion to be steadily maintained. Both the North and South American continents are located between the Atlantic Ocean and thePacific Ocean, the coastline of the North American continent is longer than that of the South American continent, and the two continents have greater longitudinal than latitudinal extents. The final horizontal force for the South American continent, as shown in Table 2, is 1.6222×10^{17} N, and the geometric features of these two continents allow us to estimate a final horizontal force of 4.0×10^{17} N for the North American continent. We assume 30% of this force is finally transformed into the push force F_{PN}. Most of the North American plate moves away from the Mid-Atlantic Ridge and in an approximately southwest direction. We assume the push force F_{PN} to be oriented in a southwest direction, with an orientation of approximately 190° with respect to latitude. Referring to Table 2, the final horizontal force for the Australian plate is 2.9162×10^{17} N, given that 30% of this force is finally transformed into the push force F_{PA}. The Australian plate moves dominantly in the northeast direction; thus, we assume the push force F_{PA} to be finally oriented in a northeast direction. The inclination of this direction to latitude is approximately 73.16°, as listed in Table 3. Subsequently, the combined force of these two forces on the Pacific plate can be written as $F_P=((F_{PN}{}^2+F_{PA}{}^2\text{-}2\times F_{PN}\times F_{PA}\times\cos(\ \text{-}\ ))^{0.5}$, where $=73.16°$ and $=10°$. The final horizontal force would be $F_P=1.6073\times10^{17}$ N, given that 90% of this force is used to drive the Pacific plate, 10% of this force is used to oppose the collisional force and shearing forces. Finally, we apply equation (2) to resolve the Pacific plate's speed, i.e., u=$F_{driving}$ y/ A, where $F_{driving}=0.9\times F_P=1.4466\times10^{17}$ N; y

is the asthenospheric thickness , y=300 km; A is the Pacific plate's area, and A=103,300,000.00 km^2. As mentioned earlier, the asthenosphere viscosity is not exactly determined and ranges from 10^{15} Pa s to 10^{20} Pa s based on various methods (e.g., laboratory experiments, glacial isostatic adjustment, and geoid modeling). This reality allows us to adopt =1.2×10^{17} Pa s. The movement's orientation is determined by the final horizontal force and may be expressed as = - and cos =($F_P{}^2$+$F_{PN}{}^2$-$F_{PA}{}^2$)/(2×F_P×F_{PN}). The calculated movement for this plate is further listed in Table 3.

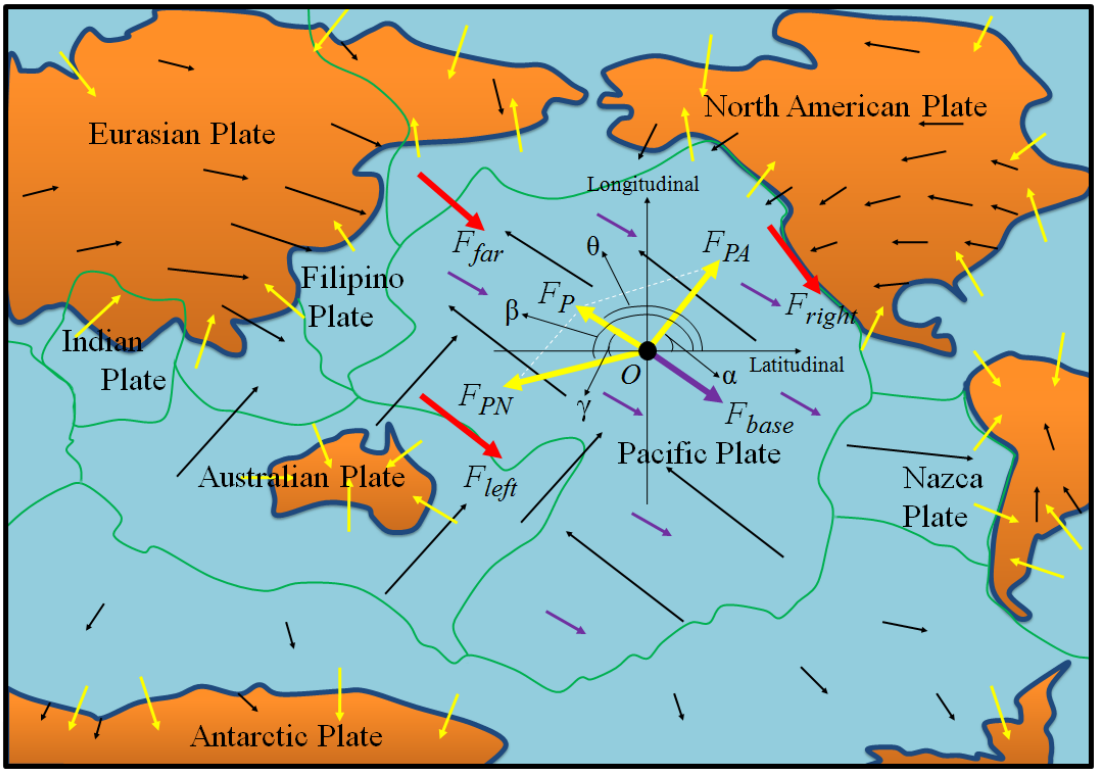

Figure 7. Modeling the dynamics of the Pacific plate. The black, yellow (thin), red, and purple (thin) arrows denote movements of plates, horizontal forces generated by oceans, resistive forces from adjacent plates, and basal friction forces, respectively. F_P, F_{PA}, and F_{PN} denote the final horizontal force exerted on the hypothetical center of geometry of the Pacific plate, the push force from the Australian plate on the hypothetical center of geometry, and the push force from the North American plate on the hypothetical center of geometry, respectively. F_{far}, F_{left}, F_{right}, and f_{base} denote the total collisional force from the part of the North American plate and the Eurasian plate , the total shearing force from the Australian plate, the total shearing force from the North American plate, and the total basal friction force exerted by the underlying asthenosphere. O denotes the hypothetical center of geometry of the Pacific plate.

, , and are the inclination of the push force F_{PA}, the push force F_{PN}, and the final horizontal force F_P to the latitudinal direction, respectively. is the angle of the push force F_{PN} and the final horizontal force F_P. Note that the push force $F_{PN}(F_{PA})$ is approximately parallel to the North American (Australian) plate's motion. The black dot denotes the hypothetical center of geometry of the plate.

The calculated and observed movements for the selected five plates are compared in Table 3. The observed movements of these plates are extracted from GSRM v.2.1 (e.g., Global Strain Rate Model) (Kreemer et al., 2014), which include more than 6739 velocities that are obtained through continuous GPS measurements. For each of these plates, the movement calculated through ocean-generated force model represents an average level of the plate, while the movement extracted from GSRM v.2.1 is a velocity measurement of individual site within the plate, to realize the comparison, we plot global plates into a grid of $10^o \times 20^o$ and use the nodes of the grid as the controlling sites of the selected five plate (Figure 8), we then extract the movements of these sites from GSRM v.2.1, these movements are further averaged. On the whole, the calculated movements are consistent with the observed movements of the selected five plates. The calculated speeds for the five plates are 21.10, 45.20, 60.90, 35.20, and 66.20 mm/yr, respectively, while the observed speeds for them are 12.33, 28.34, 56.50, 61.68, and 65.50 mm/yr. The calculated velocity orientations relative to both latitude and longitude for these plates are identical to the observed velocity orientations.

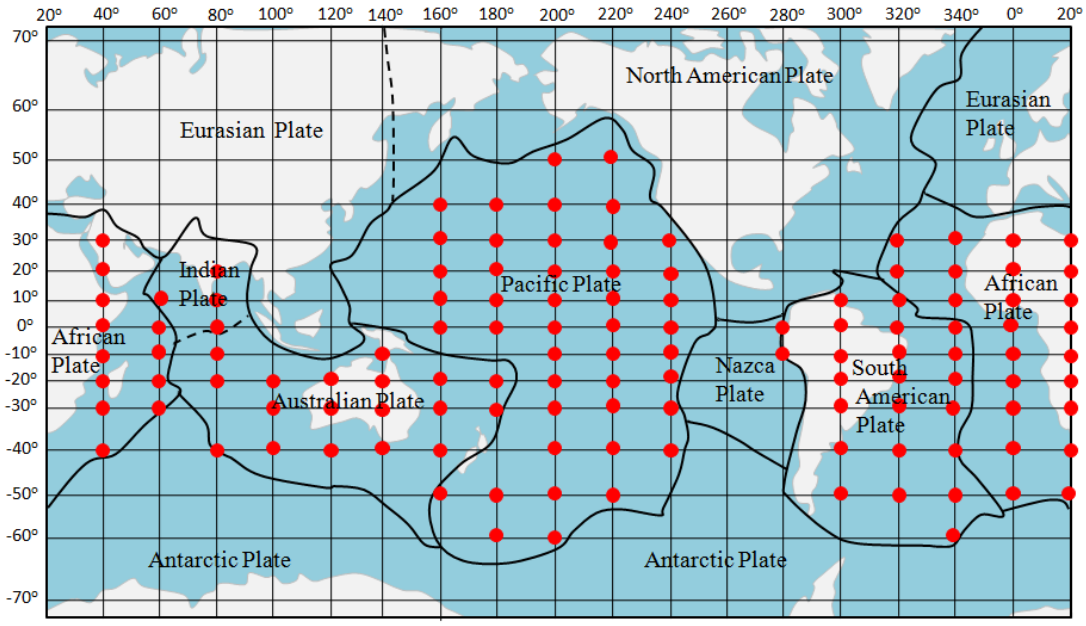

Figure 8. A global view of the controlling sites of selected five plates.

Table 3 A comparison of plate motions between ocean-generated force model and GSRM v2.1

Plate	
South American	
African	
Indian	
Australian	
Pacific	

3. 4 Resultant stress

As mentioned in section 2, the observed stresses are mainly compressional and concentrated on the uppermost part of the lithosphere (Zoback, 1992; Zoback et al., 1989; Zoback & Magee, 1991). Our modeling of the vertical distribution of horizontal stress revealed that the stress caused by slab pull cannot be in accordance with the observed stress. This failure requires other force to be responsible for the observed stresses. Ocean-generated force may be this force. Ocean is loaded on the top of the lithosphere, the region along which the ocean-generated force is exerted is topographically higher, it is easy for this force to form a stress field associated with the uppermost brittle part of the lithosphere.

A simple model is developed to demonstrate the stress produced by the ocean-generated force. The model consists the Earth's crust that is loaded with ocean. The crust is straight, and its length and height are 7,500 km and 50 km, respectively. The ocean depth varies from 5.0 km on the left to 4.0 km on the right. The crust is composed of rocks and is assumed to be homogeneous and isotropic. We employ finite element analysis software (i.e., Abaqus) to resolve the resultant stress. The model's bottom is given a remote boundary condition, and there are no edge boundary condition for the left and right ends of the model. A 50 km depth of crust represents the lithosphere's upper part, which is mostly elastic, therefore the ductile nature may be neglected. The inputs are the crust's pressure caused by its weight and the ocean's hydrostatic pressure. The outputs include two sets of data: one is the stress produced by the crust's pressure alone, and the other is the stress produced by a combination of the crust's pressure and the ocean's pressure. The two-dimensional frame allows us to obtain a horizontal stress S11 and a vertical stress S22. To realize a quantitative solution, we select the stress at 10 sites of the model to compare. The model and the resultant stress are shown in Figure 9, and the simulated stress of the selected ten sites and some of the parameters utilized in the calculation are further listed in Table 4. It can be found that ocean water has a significant impact on the crust's stress, the stress produced by ocean water is mainly compressional and penetrates the entire thickness of the crust. Along the horizontal direction, the maximal stress S11, approximately 5.4 ~ 12.5 MPa, dominates the uppermost part of the crust that is within a depth of ~ 20 km. The mean

stress of this depth is 2.7 ~ 8.04 Mpa; Along the vertical direction, the maximal stress S22, approximately 13.1 ~ 15.8 Mpa, dominates more than 40 km depth. The mean stress of this depth is 3.84 ~ 8.58 Mpa. The observed stresses (i.e., deviatoric stresses) in the upper parts of the intraplate regions have general magnitudes of 20~30 MPa (Forsyth & Uyeda, 1975; Bott and Kusznir, 1984; Zoback & Magee, 1991; Fialko et al., 2005). The deviatoric stresses in the continents are usually with the amplitude of 10 to 100 MPa (Turcotte and Schubert, 2002). In this point, the stress caused by ocean water is in accordance with the observed stress in vertical distribution, style, and amplitude. It is important to note that this model does not include collisional force and basal friction; in practice, the Earth's crust is curved, the crustal rocks are not homogeneous and isotropic, and the crust's thickness and density also vary spatially; in addition, as seen in Figure 9, the orientations of ocean-generated force are various. We expect, the stresses caused by a combination of ocean-generated force and all of these factors may realize a better match with the observed stresses in the WSM.

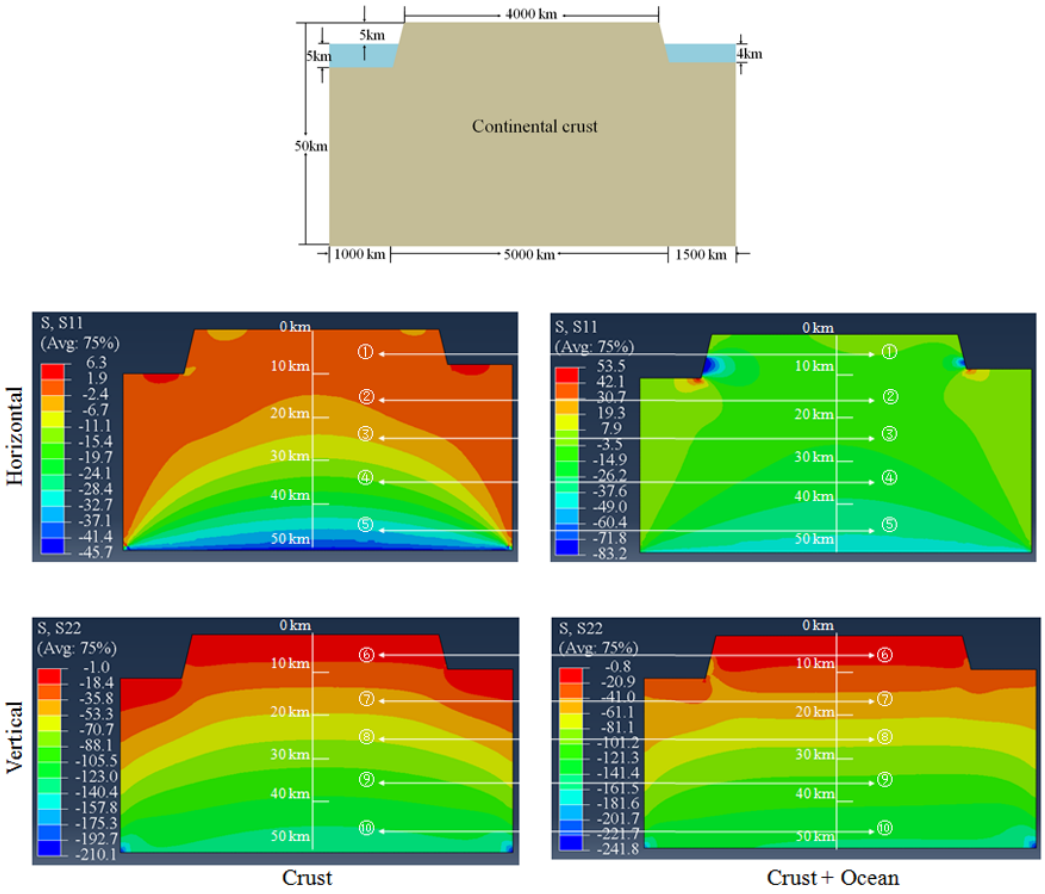

Figure 9. Modeling the stress produced by crust and ocean. Top, geometry of the model; bottom, the stress modeled by Abaqus, where the unit of stress is MPa. The negative symbol "-" denotes compressional. The numbers in the circles denote the ten selected sites in the crust.

Subsequently, a detailed investigation of the observed stress data revealed that S_{Hmax} orientations are often rotated into a plane approximately parallel to the continental slope's trend (Zoback, 1992; Zoback et al., 1989). This rotation was presently explained as a result of the superposition of stresses owing to flexure from sediment loading on the continental shelf (Dart and Zoback, 1987). Continental shelf is a part of the continent, its width is generally tens of kilometers. Sediment loading expresses mainly a weight that is added to previous topography, the stress caused by this additional weight is rather limited and very difficult to horizontally dominate the observed stresses whose orientations are subparallel and across the plate's size of thousands of kilometers length. Instead, ocean-generated force is exerted on the slope of continent, it is natural for this force to form a stress field that follows the continental slope.

Table 4 Parameters and stresses of the selected ten sites

Water's density kg/m^3	Ro kg
1,000	2,6

Note: The negative symbol "-" denotes compressional, and the positive symbol "+" denotes extensional.

4 Discussion

All continents are being surrounded by oceans, the ocean-generated forces are extensively exerted on the sides of the continents that are fixed on the top of the lithospheric plates, and all plates connect to each other, as a consequence, the interactions of all the plates may result in plate motions across the globe (Figure 10). Under the effect of ocean-generated force, a moving continental plate would ride on an oceanic plate when these two plates meet, the front part of the oceanic plate is forced to subduct, forming sinking slab; Also, a moving plate would move away from another plate, a gap forms between them. The gap, if

deep enough, allows magma to erupt, forming a MOR. As ocean-generated force is exerted on the continent's wall (represented with the coastline), the oceanic crust is extensively connected to the continental crust, this linkage allows ocean-generated force to be laterally transferred to the oceanic crust, and then, the continental crust drags the oceanic crust to lead the plate's boundary shape to follow the coastline's shape.

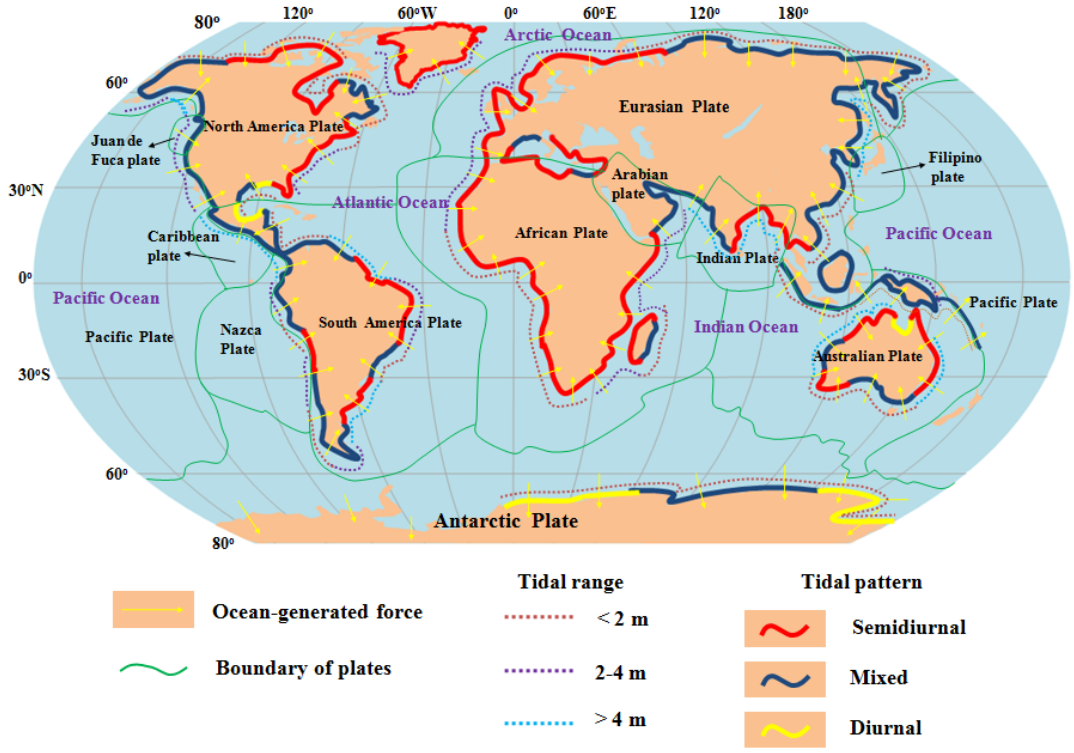

Figure 10. Global view of the distribution of plate tectonics and ocean-generated forces. The supporting tidal data are mainly from GLOSS database (e.g., the Global Sea Level Observing System) (Caldwell et al. 2015).

Although we have demonstrated in section 3 that ocean-generated force may drive plate motion, many people still oppose this force as plate driving force. Their reasons for rejecting this force include: 1) ocean constitutes just another deviation from a truly radial density distribution of the Earth. Any "lateral" density heterogeneity creates stresses that in turn lead to deformation, their extent is controlled by the rheological properties of the involved materials; 2) plate motion determines the shape of ocean basin, as a result, ocean water cannot drive plate to move; 3) ocean loading on the top of the lithosphere doesn't

allow ocean-generated force to drive the lithospheric plates to move along the asthenosphere. For instance, the water hold in a container cannot drive the bowl to move along ground; 4) ocean-generated force is too small to drive plate motion. These issues need to be clarified here. First of all, the view that any "lateral" density heterogeneity would lead denser materials (i.e., rocks) to move towards lighter materials (i.e., air or water) is rather idealized. The Himalayas is denser than the surrounding air, but it does not move by its density to reduce its height, instead, it increasingly rises. This example provides insight that a system may be disturbed to overturn the trend of "lateral" density heterogeneity. Clearly, for a system consisting of ocean water and the lithosphere it is permanently disturbed by tide, consequently, the lithospheric rocks are impossible to follow the principle of the "lateral" density heterogeneity to move towards ocean water. Indeed, plate motion may change the shape of ocean basin, but ocean water is not motionless, it may provide feedback by a dissipation of energy on plate, as a result, plate motion is affected. Ocean loading on the lithosphere is different from water loading in a container. Because the lithosphere has already fractured into individual plates, and these plates are attached to the underlying asthenosphere, this reality allows ocean-generated force to interact with the basal friction exerted by the asthenosphere on the plate. Instead, the container is perfect, the force produced by water pressure is balanced out by the container itself and cannot interact with the basal friction exerted by ground on the container. In physics, the interaction of a driving force and a resistive force is a precondition that an object moves. Figure 11 outlines how ocean-generated force apparently drives plate motion. Three plates are totally designed in the model, along the vertical direction the weight of each plate is balanced out by the supporting from the asthenosphere, thus, we just need to discuss the forces along the horizontal direction. For Plate A, as the oceanic ridge represents a boundary between the two separating plates, the ridge's crest is rift from where magma erupts, this weakness allows the ocean-generated forces F_{AR} and F_{AL}, the basal friction f_{A}, and the collisional force F_{BA} to interact with each other. Once these forces are equal in magnitude or close to each other, a force balance between these forces may be formed; For Plate B, it is assumed that Plate A rotates counterclockwise and Plate C rotates clockwise, these two plates give Plate B the collisional forces F_{AB} and F_{CB}, respectively, these two forces may also interact with the basal friction f_{B}; For Plate C, the ocean-generated forces F_{CL} and F_{CR}, the basal friction f_{C}, and the collisional force F_{BC} may also interact with each other. Subsequently, we discuss whether the force balances between these forces can be formed or not. The lithospheric plates are moving over the Earth's surface, and all plates are connected to each other, this complexity means that the magnitude of the resistive force is not easily to be known. We here provide a method to estimate the resistive force. Since all plates are attached to the underlying viscous asthenosphere, plate motion must obey the principle of fluid mechanics. The lithosphere's thickness relative to its length (i.e., area) allows the lithosphere to be treated as a "thin" shell, we assume that the whole lithosphere is steadily moving along the viscous asthenosphere, the total basal friction force exerted by the asthenosphere along the lithosphere's

base can be written as $f_{basal} = \text{Au/y}$, where , A, u, and y are the viscosity of the asthenosphere, the lithosphere's area, the lithosphere's speed, and the thickness of the asthenosphere, respectively. Given $=10^{18}$ Pa s, A=510,000,000 km^2, u=3 cm/yr, and y=300 km, then, $f_{basal} = \text{Au/y}=1.62\times10^{18}$ N. As mentioned earlier, many numerical models yield a higher viscosity of $10^{17} \sim 10^{20}$ Pa s for the asthenosphere, while laboratory experiments yield a lower viscosity down to 10^{15} Pa s for the asthenosphere, we here adopt $=10^{18}$ Pa s is appropriate. After that, the total basal friction force is allocated to individual plates based on a ratio of a plate's area and the lithosphere's area. South American, North American, African, Indian, Australian, Pacific, Eurasian, and Antarctic plates have the area of 43,600,000, 76,000,000, 61,300,000, 11,900,000, 47,000,000, 103,300,000, 67,800,000, and 60,900,000 km^2, respectively, the area ratio allows these plates to obtain a basal friction force of 1.38×10^{17} N, 2.41×10^{17} N, 1.94×10^{17} N, 3.77×10^{17} N, 1.49×10^{17} N, 3.27×10^{17} N, 2.15×10^{17} N, and 1.93×10^{17} N, respectively. Theoretically speaking, if the driving force that a plate receives is equal to this allocated basal friction force, the force balance can be formed. Table 2 shows that the ocean-generated force for South American, African, Indian, and Australian plates are 1.6222×10^{17} N, 4.8838×10^{17} N, 1.2760×10^{17} N, and 1.9162×10^{17} N, respectively. An equality in magnitude between the ocean-generated force and the allocated basal friction force allows to form force balances for these plates. Notwithstanding, plates are moving along different directions, a plate would also receive collisional force from the plate at its front, and shearing forces from the plates at its two sides, therefore, to build a force balance, all related resistive forces must be included. As these adjacent plates are also attached to the underling viscous asthenosphere, the collisional force and shearing forces that these adjacent plates provide essentially arise from the basal friction exerted by the asthenosphere on them. As seen above, each of these plates is allocated a basal friction force of $\sim10^{17}$ N. Based on the calculated ocean-generated forces in Table 2, we expect that ocean-generated forces for the continental plates would have an amplitude of $\sim10^{17}$ N. And then, we conclude each of these plates may have its own force balance, by which the motion can be steadily maintained.

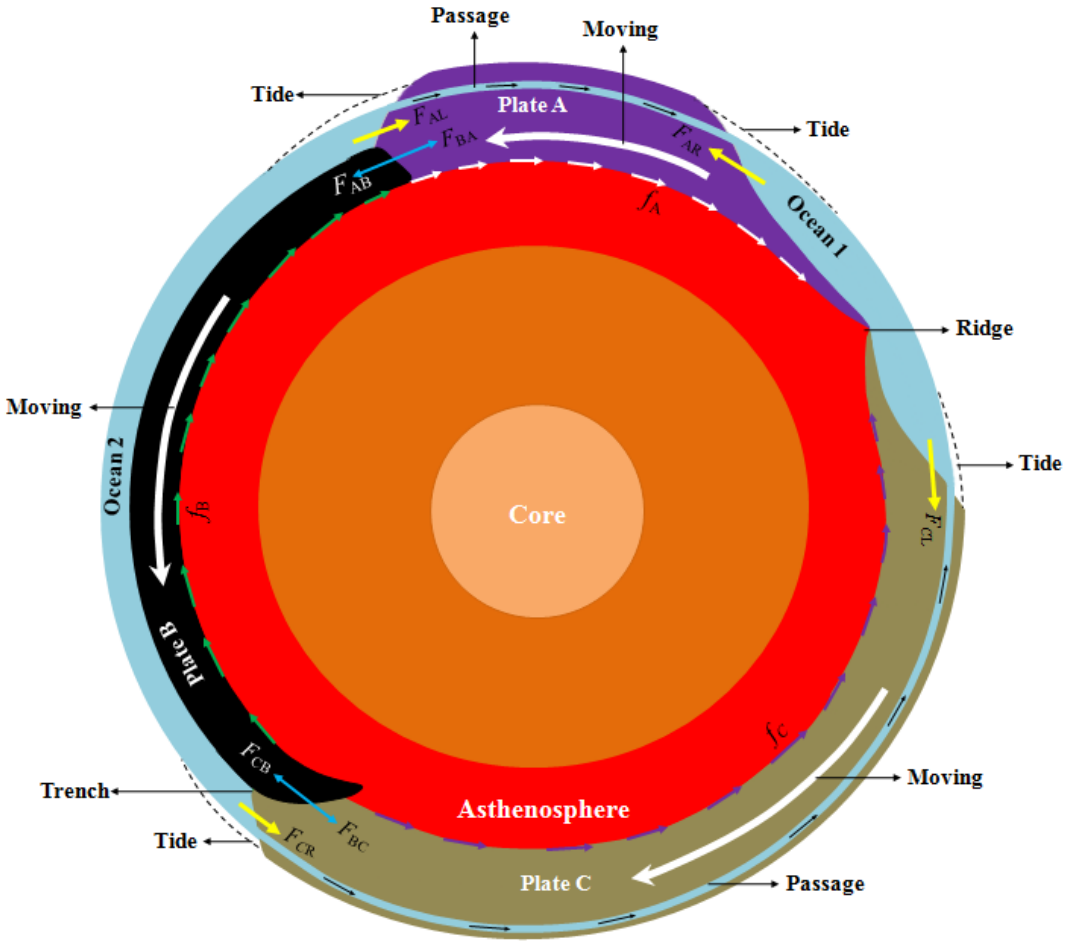

Figure 11. Modeling the dynamics of the lithospheric plates. Black arrows in the passages denote water compensation from one ocean to another. Note that the ocean depth, tide, plate size, mantle, plume, and core are highly exaggerated.

So far, we have came to a point that ocean-generated force is able to satisfy the kinematics and geometry of plate motion. Now, let's discuss how plate motion can be mechanically satisfied. As shown in Figure 11, it is assumed that the Ocean 1 depth is greater than the Ocean 2 depth. If we use a part of Ocean 2 that connects to Plate A, which is equal in length to Ocean 1, to compare, the depth difference between this part of Ocean 2 and Ocean 1 produces a net gravitational potential energy relative to the asthenosphere reference level. As Plate A and Plate B are moving away from each other, this separation would require the Ocean 1 depth to decrease as the basin elongates horizontally, and require the Ocean 2 depth to increase as the basin shortens horizontally. Conse-

quently, the net gravitational potential energy reduces. Therefore, if there were no external energy input to compensate, the net gravitational potential energy would eventually disappear terminating plate motion. Tides may be the one to supply this energy. Tides represent the regular alternations of high and low water on the Earth, when high water falls, the gravitational potential energy converts into the kinetic energy, ocean water obtains movement. As all oceans are physically connected, part of the water in Ocean 2 may travel via passages to compensate the decreasing ocean depth in Ocean 1, by which the net gravitational potential energy is sustained. Given the basal friction force f_{basal} = 1.62×10^{18} N and the movement distance u=3 cm/yr for the lithosphere, this movement distance requires an energy $Q_1 = f_{basal}\times u = 4.86\times10^{16}$ J/yr to satisfy. This energy also represents the net gravitational potential energy. Ocean water is often raised twice per day due to tide and the resultant height is given h=0.3 m. Given gravitational acceleration g=9.8 m/s, the volume v=1.35×10^9 km^3 and density =1000 kg/ m^3 for ocean water, consequently, the gravitational potential energy obtained by ocean water due to the tide's raising during a year would be Q_2=2*365* vgh=2.9×10^{21} J/yr. The transformation from gravitational potential energy to kinetic energy within ocean water and the energy transition between oceans must be complicated, we believe that a little part of this tidal energy is enough for supplying the net gravitational potential energy. In fact, the impact of tidal energy on plate motion is long discussed. Wegener (1924) presented that tides cause a slight progressive displacement of the crust. Rochester (1973) showed that the total energy released due to tidal friction exceeds $5*10^{19}$ ergs/s. These authors (e.g., Miller, 1966; Munk, 1968) concluded that the dissipation in both shallow seas and solid Earth is approximately $2*10^{19}$ ergs/s, and this amount of energy exceeds the lower bound set by seismic energy release by 2 orders of magnitude (Gutenberg, 1956) and might be available for driving plate motion. These authors (e.g., Riguzzi et al., 2010; Egbert and Ray, 2000) reevaluated the energy budget and found that the total energy released by tidal friction may reach up to $1.2*10^{20}$J/yr, and about $0.8*10^{20}$J/yr is dissipated in the oceans, shallow seas, and mantle, and the remaining energy is enough for maintaining the lithosphere's rotation, estimated at approximately $1.27*10^{19}$J/yr. Compared to these researches, this work provides another understanding: the tidal energy obtained by ocean water may feed plate motion.

The dispersal and aggregation of plates also reflect that the ocean basin had been periodically adjusted, and this change of ocean basin is often called the Wilson Cycle (Wilson, 1963). Figure 12 outlines how such a cycle may be realized. It is assumed that the left end of the model is connected to its right end, and that the Ocean 1 depth is greater than Ocean 2 depth. This ocean depth difference allows to yield ocean-generated force for the continental plate. The ocean-generated force, the collisional force between the plates, and the basal friction force exerted by the asthenosphere, and combine to form force balances. At the time of t_1 and t_2, Plate A and Plate B are moving towards each other, Plate C is pushed by Plate B to move, and Plate A overrides the front end of Plate C, Ocean 2 basin is shortening, while Ocean 1 basin is elongating; At the

time of t_3, Plate A and Plate B meet together, forming an aggregation. Plate C entirely sinks and becomes disappeared, the Ocean 2 basin closes, and the force balances terminate. As the forming oceanic crusts cannot be spread away from the ridge, they gradually accumulate and finally close magma eruption, the ridge tends to die. After that, a large asteroid collides the aggregated plate violently, forming extensive fractures on the plate, one of the fractures penetrates down to the lower part of the lithospheric plate; At the time of t_4, the big fracture induces water to enter, forming a large body of water that is deeper than Ocean 1, the deeper water body yields greater ocean-generated force. The big fracture also reflects a mass loss of the upper part of the lithosphere, the isostasy would require the upper mantle to melt, the molten material rises, the aggregated plate is apparently divided into Plate D and Plate E. Under the effect of the ocean-generated force, the two plates tend to move away from each other; At the time of t_5, a combination of the ocean-generated force and the rising molten material finally breaks the thickness of the plate, the new force balances are built, by which Plate D and Plate E move away from each other. A new oceanic ridge forms, and the increasingly separation between the two plates results in Ocean 3 basin. As the left end of the model is connected to its right end, the increasingly separation would also require the left part of Plate D to compress the right part of Plate E, together with the basal friction exerted by the asthenosphere on the plate, the left part of Plate D is eventually detached from the plate, forming subduction. Asteroid impacts are frequent events in the solar system, it is widely believed that the initiation of plate motion relates to large asteroid impact (Alvarez, et al., 1980; Rampino and Stothers, 1984; Prinn and Fegley, 1987; Marzoli, et al., 1999; Hames, et al., 2000; Condie, 2001; Wan, 2018), but the detail of this coupling remains elusive. Our demonstration here provides first insight on this issue: asteroid impact initiates plate motion, ocean water yields force to maintain plate motion, and tide provides energy for plate motion.

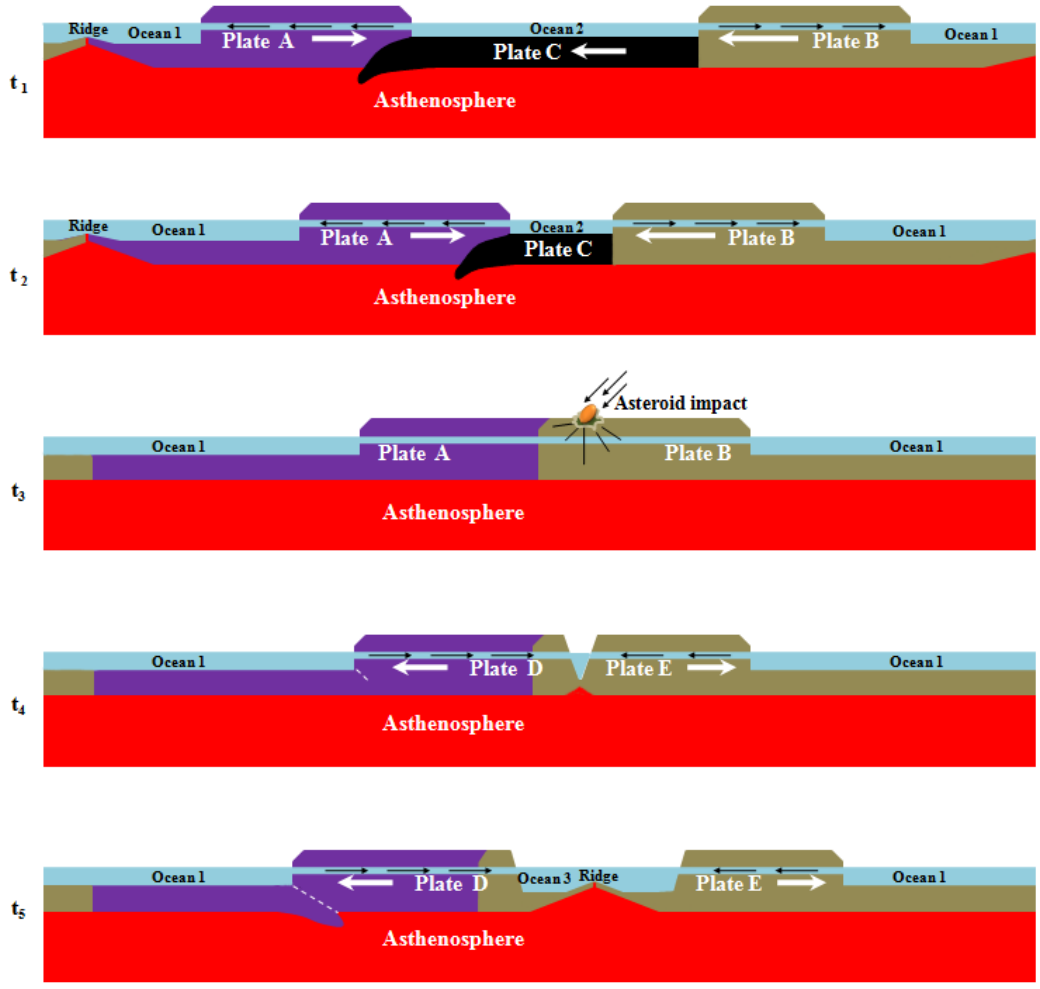

Figure 12. Modeling the dispersal and aggregation of plates. Back arrows in the passages denote water compensation from one ocean to another. Note that the ocean depth, plate size, and mantle are highly exaggerated.

Many people are extraordinarily perplexed as to why the Earth owns plate tectonics whereas the Venus does not. A lot of researches have shown that water provides the right conditions (maintaining a cool surface, for example) for plate tectonics, while the water's absence on Venus prohibits plate formation (Driscoll and Bercovici, 2013; Hilairet et al., 2007; Lenardic et al., 2008; Korenaga, 2007; Tozer, 1985; Lenardic and Kaula, 1994; Hirth and Kohlstedt, 1996; Landuyt and Bercovici, 2009). Our understanding of the kinematics and mechanics of ocean water provides additional solution to this issue: no water on Venus means no

the contribution of ocean-generated force, and further no development of plate tectonics on the planet.

Acknowledgments

We express sincere thanks to Jinmin Chen for conducting the analysis of vector force and also to Bernhard Steinberger, Jeroen van Hunen, Maureen D. Long, and Thorsten Becker for their helpful comments on this research. The author declares that there is no conflict of interest. No funding is provided for this research.

Data Availability Statement

The data used for this study are already included in the text of this paper.

References

Alvarez, L. W., Alvarez, W., Asaro, F., and Michel, H. V. (1980). Extraterrestrial cause for the Cretaceous-Tertiary extinction. *Science*, 208,1095-1108.

Amante, C., and Eakins, B. W. (2009). ETOPO1 1 Arc-Minute Global Relief Model: Procedures, Data Sources and Analysis. NOAA Technical Memorandum NESDIS NGDC-24. National Geophysical Data Center, NOAA. doi:10.7289/V5C8276M.

Alisic, L., Gurnis, M., Stadler, G., Burstedde, C., and Ghattas, O. (2012). Multi-scale dynamics and rheology of mantle flow with plates. *J. Geophys. Res.*, 117, B10402, doi:10.1029/2012JB009234.

Becker, T. W., Faccenna, C. (2011). Mantle conveyor beneath the Tethyan collisional belt: Earth Planet. *Sci. Lett.*, 310, 453-461.

Becker, T. W., and O'Connell, R. J. (2001). Predicting plate velocities with mantle circulation models. *Geochem. Geophys. Geosyst.*, 2, 2001GC000171.

Becker, T. W. (2017). Superweak asthenosphere in light of upper mantle seismic anisotropy. *Geochem. Geophys. Geosyst.*, 18, doi:10.1002/ 2017GC006886.

Bercovici, D., Tackeley, P. J., and Ricard, Y. (2015). The generation of plate tectonics from mantle dynamics: Reference Module in Earth Systems and Environmental Science. *Treatise on Geophysics (Second Edition)*, 7, 271-318.

Berner. R. (2004). The Phanerozoic Carbon Cycle, Oxford University Press.

Bird, P., Liu, Z., Rucker, W. K. (2008). Stresses that drive the plates from below: definitions, computational path, model optimization, and error analysis. *J. Geophys. Res.*, 113, B11406.

Bokelmann, G. H. R. (2002). Which forces drive North America? *Geology*, 30, 1027-1030.

Bott, M. H. P. (1993). Modeling the Plate-Driving Mechanism. *Journal of the Geological Society*, 150, 941-951.

Bott, M. H. P., Kusznir, N. J. (1984). The origin of tectonic stress in the lithosphere. *Tectonophysics*, 105, 1-13.

Brandmayr, E., Marson, I., Romanelli, F., & Panza, G. F. (2011). Lithosphere density model in Italy: no hint for slab pull. *Terra Nova*, 23, 292-299.

Cande, S. C., LaBrecque, J. L., Larson, R. L., Pitman, W. C., III, Golovchenko, X., and Haxby,W. F. (1989). Magnetic lineations of the world's ocean basins, Tulsa, Oklahoma. American Association of Petroleum Geologists.

Cande, S. C., Kent, D. V. (1992). A new geomagnetic polarity time scale for the Late Cretaceous and Cenozoic. *J. Geophys. Res.*, 97(10), 13917-13951.

Caldwell, P. C., Merrfield, M. A., Thompson, P. R. (2015). Sea level measured by tide gauges from global oceans - the Joint Archive for Sea Level holdings (NCEI Accession 0019568), Version 5.5, NOAA National Centers for Environmental Information, Dataset, doi:10.7289/V5V40S7W.

Chapple, W. M., and Tullis, T. E. (1977). Evaluation of the forces that drive the plates. *J. Geophys. Res.*, 82, 1969-1984.

Cloetingh, S., and Wortel, R. (1986). Stress in the Indo-Australian plate. *Tectonophysics*, 132, 49-67.

Coltice, N., Gerault, M., and Ulvrova, M. (2017). A mantle convection perspective on global tectonics. *Earth-Science Reviews*, 165, 120-150.

Condie, K. C. (2001). Mantle plumes and their record in Earth history. Cambridge University Press, Cambridge.

Conrad, C. P., Hager, B. H. (1999). The effects of plate bending and fault strength at subduction zones on plate dynamics. *J. Geophys. Res.*, 104, 17551-17571.

Conrad, C. P., Lithgow-Bertelloni, C. (2002). How Mantle Slabs Drive Plate Tectonics. *Science*, 298 (5591), 207-09.

Conrad, C. P., & Lithgow-Bertelloni, C. (2003). How mantle slabs drive plate tectonics. *Science*, 298, 207-209.

Cruciani, C., Carminati, E., & Doglioni, C. (2005). Slab dip vs. lithosphere age: no direct function. *Earth and Planetary Science Letters*, 238, 298-310.

Dart, T. L., Zoback, M. L. (1987). *US Open File Rep.*, 43, 87-283.

Doglioni, C., Ismail-Zadeh, A., Panza, G., Riguzzi, F. (2011). Lithosphere-asthenosphere viscosity contrast and decoupling. *Physics of the Earth and Planetary Interiors*, 189, 1-8.

Doglioni, C., and Panza, G. (2015). Polarized Plate Tectonics. *Advances in Geophysics*, 56,1-167.

Driscoll, P. and Bercovic, D. (2013). Divergent evolution of Earth and Venus: Influence of degassing, tectonics, and magnetic fields. *Icarus*, 226, 1447-1464.

Egbert, G. D., Ray, R. D. (2000). Significant dissipation of tidal energy in the deep ocean inferred from satellite altimeter data. *Nature*, 405, 775-778.

El Gabry, M. N., Panza, G. F., Badawy, A. A., & Korrat, I. M. (2013). Imaging a relic of complex tectonics: the lithosphere-asthenosphere structure in the Eastern Mediterranean. *Terra Nova*, 25(2), 102-109.

Faccincani, L., Faccini, B., Casetta, F., Mazzucchelli, M., Nestola, F., Coltorti, M. (2021), EoS of mantle minerals coupled with composition and thermal state of the lithosphere: Inferring the density structure of peridotitic systems. *Lithos*, 404-405, 106483.

Fleitout, L., Froidevaux, C. (1983). Tectonic stresses in the lithosphere. *Tectonics*, 2(3), 315-324.

Forsyth, D. & Uyeda, S. (1975). On the relative importance of the driving forces of plate motion. *Geophys. J. Int.*, 43, 163-200.

Freed, A., Hashima, A., Becker,T. W., Okaya, D. A., Sato, H., and Hatanaka, Y. (2017). Resolving depth-dependent subduction zone viscosity and afterslip from postseismic displacements following the 2011 Tohoku-oki, Japan earthquake. *Earth Planet. Sci. Lett.*, 459, 279-290.

Frepoli, A., Selvaggi, G., Chiarabba, C., & Amato, A. (1996). State of stress in the Southern Tyrrhenian subduction zone from fault-plane solutions. *Geophysical Journal International*,125, 879-891.

Ghosh, A., Becker, T. W., Humphreys, E. D. (2013). Dynamics of the North American continent. *Geophys. J. Int.*, 194, 651-669.

Ghosh, A., and Holt, W. E. (2012). Plate motions and stresses from global dynamic models. *Science*, 335, 839-843.

Gölke, M., and Coblentz, D. (1996). Origins of the European regional stress field. *Tectonophysics*, 266, 11-24.

Gripp, A. E., & Gordon, R. G. (2002). Young tracks of hotspots and current plate velocities. *Geophysical Journal International*, 150, 321-361.

Grünthal, G., and Stromeyer, D. (1992). The recent crustal stress field in central Europe: Trajectories and finite element modeling. *J. Geophys. Res.*, 97(B8), 11, 805-11,820.

Gutenberg, B. (1956). The energy of Earthquakes. *Quart. J. Geol. Soc. London*, 112, 1-14.

Hager, B. H., and Richards, M. A. (1989). Long-wavelength variations in Earth's geoid: Physical models and dynamical implications. *Philosophical Transactions of the Royal Society of London, Series A*, 328, 309-327.

Hales, A. (1936). Convection currents in the Earth. *Monthly Notice of the Royal Astronomical Society, Geophysical Supplement*, 3, 372-379.

Hames, W. E., Renne, P. R., Ruppel, C. (2000). New evidence for geologically instantaneous emplacement of earliest Jurassic Central Atlantic magmatic province basalts on the North American margin. *Geology*, 28,859-862.

Hawley, W. B., Allen, R., and Richards, M. A. (2016). Tomography reveals buoyant asthenosphere accumulating beneath the Juan de Fuca plate. *Science*, 353, 1406-1408.

Heidbach, O., Rajabi, M., Cui , X. F., Fuchs, K., Müller, B., Reinecker, J., Reiter, K.,Tingay., M., Wenzel, F., Xie, F. R., Ziegler, M. O., Zoback, M., Zoback, M. (2018). The World Stress Map database release 2016: Crustal stress pattern across scales. *Tectonophysics*, 744, 484-498.

Heidbach, O., Reinecker, J., Tingay, M., Müller, B., Sperner, B., Fuchs, K., Wenzel, F. (2007). Plate boundary forces are not enough: Second- and third-order stress patterns highlighted in the World Stress Map database. *Tectonics*, 26, http://doi.org/10.1029/2007TC002133 (PDF).

Heidbach, O., Tingay, M., Barth, A., Reinecker, J., Kurfeß, D., Müller, B. (2010). Global crustal stress pattern based on the World Stress Map database release 2008. *Tectonophys*, 482, 3-15.

Heidbach, O., Rajabi, M., Reiter, K., Ziegler, M. (2016). World Stress Map 2016. GFZ Data Services, http://doi.org/10.5880/WSM.2016.002.

Hess, H. H. (1962). History Of Ocean Basins, in Engel, A. E. J., James, H. L., & Leonard, B. F., eds. Petrologic Studies: A volume in honor of A. F. Buddington. Boulder, CO, *Geological Society of America*, 599-620.

Hibsch, C., Jarrige, J-J., Cushing, E. M., Mercier, J. (1995). Paleostress analysis, a contribution to the understanding of basin tectonics and geodynamic evolution: example of the permian-cenozoic tectonics of Great Britain and geodynamic implications in Western Europe. Tectonophysics, 252, 103-136.

Hilairet, N., Reynard, B., Wang, Y., et al.:

Hirth, G. and Kohlstedt, D. (1996). Water in the oceanic upper mantle: Implications for rheology, melt extraction and the evolution of the lithosphere. *Earth and Planetary Science Letters*, 144, 93-108.

Holmes, A. (1931). Radioactivity and Earth Movements. *Nature*, 128, 496-496.

Holtzman, B. (2016). Questions on the existence, persistence, and mechanical effects of a very small melt fraction in the asthenosphere. *Geochem. Geophys. Geosyst.*, 17, 470-484, doi:10.1102/2015GC006102.

Hu, Y., Bürgmann, R., Banerjee, P., Feng, L. J., Hill, E. M., Ito, T., Tabei, T., Wang, K. L. (2016). Asthenosphere rheology inferred from observations of the 2012 Indian Ocean earthquake. *Nature*, 538(7625), 368-372.

Isacks, B., & Molnar, P. (1971). Distribution of stresses in the descending lithosphere from a global survey of focal-mechanism solutions of mantle earthquakes.

Reviews of Geophysics, 9, 103-174.

James, T. S., Gowan, E. J., Wada, L., and Wang, K. L. (2009). Viscosity of the asthenosphere from glacial isostatic adjustment and subduction dynamics at the northern Cascadia subduction zone, British Columbia, Canada. *Journal of Geophysical Research: Solid Earth*, 114(B4), CiteID B04405.

Jordan, T. H. (1974). Some comments on tidal drag as a mechanism for driving plate motions. *J. Geophys. Res.*, 79, 2141-2142.

Kaufmann, G., and Lambeck, K. (2000). Mantle dynamics, postglacial rebound and the radial viscosity profile. *Physics of the Earth and Planetary Interiors*, 121, 301-324.

Kawakatsu, H., Kumar, P., Takei,Y., Shinohara, M., Kanazawa, T., Araki, E., and Suyehiro, K. (2009). Seismic evidence for sharp lithosphere asthenosphere boundaries of oceanic plates. *Science*, 324, 499-502.

Kido, M., Yuen, D. A., Cadek, O., and Nakakuki, T. (1998). Mantle viscosity derived by genetic algorithm using oceanic geoid and seismic tomography for whole mantle versus blocked-flow situations. *Physics of the Earth and Planetary Interiors*, 107, 307-326.

King, S. D. (1995). The viscosity structure of the mantle, In Reviews of Geophysics (Supplement) U.S. *Quadrennial Report to the IUGG* 1991-1994, 11-17.

Korenaga, J. (2007). Thermal cracking and the deep hydration of oceanic lithosphere: A key to the generation of plate tectonics?. *J. Geophys. Res.*, 112(B5), DOI: 10.1029/2006JB004502.

Korenaga, J., Karato, S.-I. (2008). A new analysis of experimental data on olivine rheology. *J. Geophys. Res.*, 113, B02403.

Kreemer, C., Blewitt, G., and Klein, E.C. (2014). A geodetic plate motion and Global Strain Rate Model. *Geochemistry, Geophysics, Geosystems*, 15, 3849-3889.

Kreemer, C., Holt, W. E., & Haines, A. J. (2002). The global moment rate distribution within plate boundary zones. *American Geophysical Union Geodynamics Series*, 30, 173-189.

Kusznir, N. J., & Bott, M. H. P. (1977). Stress concentration in the upper lithosphere caused by underlying viscoelastic creep. *Tectonophysics*, 43, 247-256.

Landuyt, W. and Bercovici, D. (2009). Variations in planetary convection via the effect of climate on damage. *Earth and Planetary Science Letter*, 277, 29-37.

Lenardic, A., Jellinek, M., and Moresi, L-N. (2008). A climate change induced transition in the tectonic style of a terrestrial planet. *Earth and Planetary Science Letters*, 271, 34-42.

Lenardic, A. and Kaula, W. (1994). Self-lubricated mantle convection: Two-dimensional models. *Geophysical Research Letters*, 21, 1707-1710.

Lithgow-Bertelloni, C., Richards, M. A. (1995). Cenozoic plate driving forces. *Geophys. Res. Lett.*, 22, 1317-1320.

Lithgow-Bertelloni, C. (2014). Driving Forces: Slab Pull, Ridge Push. Encyclopedia of Marine Geosciences.

Ma, Z. J., Li, C. D., Gao, X. L. (1996). General characteristics of global tectonics in the Mesozoic and Cenozoic (in Chinese). *Geological Science and Technology Information*, 15(4), 21-25.

Marzoli, A., Renne, P. R., Piccirillo, E. M., Ernesto, M., Bellieni, G., de Min, A. (1999). Extensive 200-million-year-old continental flood basalts of the Central Atlantic magmatic province. *Science*, 284(5414),616-618.

McKenzie, D. P. (1968). The Influence of the Boundary Conditions and Rotation on Convection in the Earth's Mantle. *The Geophysical Journal*, 15, 457-500.

McKenzie, D. P. (1969). Speculations on the Consequences and Causes of Plate Motions. *The Geophysical Journal*, 18, 1-32.

Mei, S., Bai, W., Hiraga, T., and Kohlstedt, D. L. (2002). Influence of melt on the creep behavior of olivine basalt aggregates under hydrous conditions. *Earth and Planetary Science Letters*, 201, 491-507.

Middleton, G. V., Wilcock, P. R. (1996). Mechanics in the Earth and Environmental Sciences, Cambridge University Press, Australia , 496.

Miller, G. R. (1996). The flux of tidal energy out of the deep oceans. *J. Geophys. Res.*, 71, 2485-2489.

Mitrovica, J. X. (1996). Haskell (1935) revisited. *J. Geophys. Res.*, 101, 555-569.

Mojzsis, S. J., Harrison, T. M., and Pidgeon, R. T. (2001). Oxygen-isotope evidence from ancient zircons fro liquid water at the Earth's surface 4,300 Myr ago. *Nature*, 409(6817):178-181.

Morgan, W. J. (1972). Deep mantle convection plumes and plate motions. *Bull. A. Pet. Geol.*, 56, 203-213.

Müller, B., Zoback, M. L., Fuchs, K., Mastin, L., Gregersen, S., Pavoni, N., Stephansson, O., Ljunggren, C. (1992). Regional patterns of tectonic stress in Europe. *J. Geophys. Res.*, 97(B8), 11,783-11,803.

Munk, W. (1968). Once again-tidal friction. *Quarterly Journal of the Royal Astronomical Society*, 9, 352-375.

Naif, S., Key, K., Constable, S., and Evans, R. L. (2013). Melt-rich channel observed at the lithosphere-asthenosphere boundary. *Nature*, 495, 356-359.

Naliboff, J. B., Lithgow-Bertelloni, C., Ruff, L. J., de Koker, N. (2012). The effects of lithospheric thickness and density structure on Earth's stress field. *Geophysical Journal International*, 188, 1-17.

Oxburgh, E. and Turcotte, D. (1978). Mechanisms of continental drift. *Reports on Progress in Physics*, 41, 1249-1312.

Panza, G. F., Peccerillo, A., Aoudia, A., & Farina, B. (2007). Geophysical and petrological modeling of the structure and composition of the crust and upper mantle in complex geodynamic settings: the Tyrrhenian Sea and surroundings. *Earth-Science Reviews*, 80, 1-46.

Parsons, B., Richter, F. M. (1980). A relation between the driving force and geoid anomaly associated with mid-ocean ridges. *Earth and Planetary Science letters*, 51, 445-450.

Perkeris, C. (1935). Thermal convection in the interior of the Earth. *Monthly Notices of the Royal Astronomical Society, Geophysical Supplement*, 3, 343-367.

Pollitz, F. F., Bürgmann, R., & Romanowicz, B. (1998). Viscosity of oceanic asthenosphere inferred from remote triggering of earthquakes. *Science*, 280, 1245-1249.

Prinn, R. G., Fegley, B. (1987). Bolide impacts, acid rain, and biospheric traumas at the Cretaceous-Tertiary boundary. *Earth and Planetary Science Letters*, 83,1-15.

Raymond, C. A., Stock, J, M., Cande, S. C. (2000). Fast Paleogene motion of the Pacific hotspots from revised global plate circuitcon straints. *Geophysical Monography*, 121, 359-375.

Rampino, M. R., Stothers, R. B. (1984). Geological rhythm and cometary impacts. Sciences, 226(4681),1427-1431.

Reynard, B., Hilairet, N., Wang, Y., Daniel, I., Merkel, S., Petitgirard, S., Nishiyama, N. (2007). High-pressure creep of serpentine, interseismic deformation, and initiation of subduction. *Science*, 318(5858), 1910-1913.

Ricard, Y., Fleitout, L., Froidevaux. C. (1984). Geoid heights and lithospheric stresses for a dynamic earth. *Ann. Geophys*, 2, 267- 286.

Richardson, R. M. (1992). Ridge Forces, Absolute Plate Motions, and the Intraplate Stress Field. *J. Geophys. Res.*, 97, 11739-11748.

Richardson, R. M., and Cox, B. L. (1984). Evolution of oceanic lithosphere: A driving force study of the Nazca Plate. *Journal of Geophysical Research: Solid Earth*, 89 (B12), 10043-10052.

Richardson, R. M., and Reding, L. (1991). North American plate dynamics. *J. Geophys. Res.*, 96, 12201-12223.

Richardson, R. M., Solomon, S. C., and Sleep, N. H. (1979). Tectonic stress in the plates. *Rev. Geophys.*, 17, 981-1019.

Riguzzi, F., Panza, G., Varga, P., Doglioni, C. (2012). Can Earth's rotation and tidal despinning drive plate tectonics?. *Tectonophysics*, 484, 60-73.

Rochester, M. G. (1973). The Earth's rotation. *EOS, T rans. Am. geophys. Un.*, 54, 769-780.

Runcorn, S. (1962a). Towards a theory of continental drift. *Nature*, 193, 311-314.

Runcorn, S. (1962b). Convection currents in the Earth's mantle. *Nature*, 195, 1248-1249.

Russo, R. M., & Silver, P. G. (1994). Trench-parallel flow beneath the Nazca plate from seismic anisotropy. *Science*, 263, 1105-1111.

Scoppola, B., Boccaletti, D., Bevis, M., Carminati, E., Doglioni, C. (2006). The westward drift of the lithosphere: A rotational drag?. *GSA Bulletin*, 118, 199-209.

Slomon, S. C., Sleep, N. H., and Richardson, R. M. (1975). On the forces driving plate tectonics: Inferences from absolute plate velocities and intraplate stress. *Geophys. J. R. Astron. Soc.*, 42, 769-801.

Spence, W. (1987). Slab pull and the seismotectonics of subducting lithosphere. *Reviews of Geophysics*, 25 (1), 55-69.

Sperner, B., Müller, B., Heidbach, O., Delvaux, D., Reinecker, J., Fuchs, K. (2003). Tectonic stress in the Earth's crust: advances in the World Stress Map project, in New insights in structural interpretation and modelling, edited by D. A. Nieuwland, Special Publication 212, 101-116, Geol. Soc. Spec. Pub., London.

Stadler, G., Gurnis, M., Burstedde, C., Wilcox, L. C., Alisic, L., Ghattas, O. (2010). The dynamics of plate tectonics and mantle flow: from local to global scales. *Science*, 329, 1033-1038.

Stefanick, M., and Jurdy, D. M. (1992). Stress observations and driving force models for the South American plate. *J. Geophys. Res.*, 97, 11905-11913.

Stern, T. A., Henrys, S. A., Okaya, D., Louie, J. N., Savage, M. K., Lamb, S., Sato, H., Sutherland, R., and Iwasak, T. (2015). A seismic reflection image for the base of a tectonic plate. *Nature*, 518, 85-88.

Steinberger, B., Schmeling, H., Marquart, G. (2001). Large-scale lithospheric stress field and topography induced by global mantle circulation. *Earth Planet. Sci. Lett.*, 186, 75-91, doi:10.1016/S0012-821X(01)00229-1

Steinberger, B. (2016). Topography caused by mantle density variations: observation-based estimates and models derived from tomography and lithosphere thickness. *Geophys. J. Int.*, 205, 604-621.

Tanimoto, T., Lay, T. (2000). Mantle dynamics and seismic tomography. *Proceedings of the National Academy of Sciences*, 97 (23), 12409-12410.

Tozer, D. (1985). Heat transfer and planetary evolution. *Geophysical Surveys*, 7, 213-246.

Turcotte, D. L., and Oxburgh, E. (1972). Mantle convection and the new global tectonics. *Annual Review of Fluid Mechanics*, 4, 33-66.

Turcotte, D. L., & Schubert, G. (2002). Geodynamics. Cambridge University Press, Cambridge.

Turcotte, D. L., Schubert, G. (2014). Geodynamics (Third Edition), Cambridge University Press, Cambridge.

Tutu, A. O., Steinberger, B., Sobolev, S. V., Rogozhina, I., Popov, A. A. (2018). Effect of upper mantle heterogeneities on lithospheric stress field and dynamic topography. *Solid Earth*, 9, 649-668, doi:10.5194/se-9-649-2018

Ulmer, P., & Trommsdorff, V. (1995). Serpentine stability to mantle depths and subduction related magmatism. *Science*, 268, 858-861.

Valley, J. W., Peck, W. H., King, E. M., and Wilde, S. A. (2002). A cool early earth. *Geology*, 30(4): 351-354.

Vigny, C., Ricard, Y., Froidevaux, C. (1991). The Driving Mechanism of Plate Tectonics. *Tectonophysics*, 187, 345-360.

Vine, F. J., & Matthews, D. H. (1963). Magnetic Anomalies Over Oceanic Ridges. *Nature*, 199, 947-949.

Walker, J., Hays, J., and Kasting, J. (1981). A negative feedback mechanism for the long-term stabilization of Earth's surface temperature. *J. Geophys. Res.*, 86: 9776-9782.

Wan, T. F. (1993). Tectonic stress field and its application to the intraplate in Eastern China (in Chinese). Beijing, Geological Publishing Company, 1-103.

Wan, T. F. (2018). On the dynamic mechanics of global lithosphere plate tectonics (In Chinese). *Earth Science Frontiers*, 25, DOI:10.13745/j.esf.sf.2018.1.1.

Wegener, A. (1915). The Origin of Continents and Oceans, New York, NY, Courier Dover Publications.

Wegener, A. (1924). The origin of continents and oceans (Entstehung der Kontinente und Ozeane), Methuen & Co.

White, R., McKenzie, D. (1989). Magmatism at rift zones: The generation of volcanic continental margins and flood basalts. *J. Geophys. Res.*, 94, 7685-7729.

Wilson, J. T. (1963). A possible origin of the Hawaiian Island. *Canada Journal of Physics*, 41, 863-868.

Wortel, R., and Cloetingh, S. (1981). On the origin of the Cocos-Nazca spreading center. *Geology*, 9, 425-430.

Zhong, S. (2001). Role of ocean-continent contrast and continental keels on plate motion, net rotation of lithosphere, and the geoid. *J. Geophys. Res.*, 106, 703-712.

Zoback, M. L., and Burke, K. (1993). Lithospheric stress patterns: A global view. Eos Trans. AGU, 74, 609-618.

Zoback, M. L., Zoback, M. D., Adams, J., Assumpção, M., Bell, S., Bergman, E. A., Blümling, P., Brereton, N. R., Denham, D., Ding, J., Fuchs, K., Gay, N., Gregersen, S., Gupta, H. K., Gvishiani, A., Jacob, K., Klein, R., Knoll, P., Magee, M., Mercier, J. L., Müller, B. C., Paquin, C., Rajendran, K., Stephansson, O., Suarez, G., Suter, M., Duias, A., Xu, Z. H., Zhi, Z. M. (1989). Global patterns of tectonic stress. *Nature*, 341, 91-298.

Zoback, M. L., Magee, M. (1991). Stress magnitudes in the crust: constraints from stress orientation and relative magnitude data. *Philosophical Transactions of the Royal Society, London*, A337(1645), 181-194.

Zoback, M. L. (1992). First- and Second-Order Patterns of Stress in the Lithosphere: The World Stress Map Project. *J. Geophys. Res.*, 97(B8), 11703-11728.

Zoback, M. D., and Zoback, M. L. (1991). Tectonic stress field of North America and relative plate motions, In Neotectonics of North America, Decade Map vol. I, edited by D. B. Slemmons et al., 339-366, Geol. Soc. of Am., Boulder, Colo.